

An Efficient Sequential Approach for k -Parametric Dynamic Generalised Linear Models

Mariane B. Alves^{*†}, Helio S. Migon^{*}, Silvano V. dos Santos Jr.^{*}, Raíra Marotta^{*}

^{*}Instituto de Matemática, Universidade Federal do Rio de Janeiro, Rio de Janeiro, Brazil.

[†]Address for correspondence: Mariane B. Alves, Universidade Federal do Rio de Janeiro, Av. Athos da Silveira Ramos, 149 - Edifício do Centro de Tecnologia, Bloco C (Térreo), Rio de Janeiro, 21941-909, Brazil. E-mail: mariane@im.ufrj.br.

January 15, 2025

Abstract

A novel sequential inferential method for Bayesian dynamic generalised linear models is presented, addressing both univariate and multivariate k -parametric exponential families. It efficiently handles diverse responses, including multinomial, gamma, normal, and Poisson distributed outcomes, by leveraging the conjugate and predictive structure of the exponential family. The approach integrates information geometry concepts, such as the projection theorem and Kullback-Leibler divergence, and aligns with recent advances in variational inference. Applications to both synthetic and real datasets highlight its computational efficiency and scalability, surpassing alternative methods. The approach supports the strategic integration of new information, facilitating monitoring, intervention, and the application of discount factors, which are typical in sequential analyses. The R package `kDGLM` is available for direct use by applied researchers, facilitating the implementation of the method for specific k -parametric dynamic generalised models.

Keywords: Bayesian analysis, Dynamic models, Information geometry, Monitoring and intervention, Sequential analysis.

1 Introduction

In practical applications, modelling time series via multi-parametric Gaussian and non-Gaussian distributions is a common objective, as described by Cargnoni et al. (1997); da Silva et al. (2011); Gamerman et al. (2013); Souza et al. (2016); Alves et al. (2010) and Migon et al. (2013). Dynamic generalised linear models (DGLMs), introduced by West et al. (1985), extend generalised linear models (GLM, Nelder and Wedderburn, 1972) and dynamic linear models (Harrison and Stevens, 1976), providing responses with temporal autocorrelation defined in the uniparametric exponential family. Our study extends DGLMs to k -parametric ($k \geq 1$), univariate, or multivariate exponential family responses, enabling sequential Bayesian inference with low computational cost, facilitating online monitoring and intervention, along with other typical facilities of Bayesian dynamic modelling.

The proposed method allows the use of k dynamic predictors, providing flexibility and temporal dynamics to the predictive structure of all parameters characterizing the observational model, with the potential to incorporate trends, seasonality, regressor effects, and more, in each predictor. It is possible to specify dynamic evolution for all structural components in these predictors. Based on information geometry elements (Amari, 2016), our method preserves sequential updating in Bayesian learning while handling structural uncertainty. Computational efficiency is achieved in part by conjugate and predictive setups in exponential families.

We focus on dynamic models, which are structured using time-indexed observables represented as y_t for $t = 1, 2, \dots$. It is assumed that the observables are conditionally independent given latent states θ_t . Stochastic Markovian rules drive the evolution of the latent states, which guide dynamic predictors based on structural blocks like trends, seasonal patterns, covariate effects, and interventions. Under normality assumptions and additional conditions (see Migon et al., 2005, 2023, for details), Bayesian updating and retrospective analysis are analytically feasible (West and Harrison, 1997, Chap. 4). For non-Gaussian dynamic models, analytical updating is generally not possible, requiring approximations

such as Monte Carlo Markov chain (MCMC) methods, which can incur high computational costs and loss of sequential analysis (Frühwirth-Schnatter (1994); Carter and Kohn (1994); Gamerman (1998); Shephard and Pitt (1997); and Durbin and Koopman (2002)).

The foundation for our investigation is the work of Marotta (2018), which used information geometry to provide a sequential method for dynamic models with univariate, uniparametric exponential family responses. We generalise on West et al. (1985) and Marotta (2018) to include k -parametric exponential families ($k \geq 1$). Applying Bregman’s projection theorem (Amari, 2016), we minimise the divergence between canonical parameter conjugates and state-induced prior specifications. This makes it possible to execute sequential inference in dynamic models for responses with any distribution of k -parametric exponential families, such as the ones used in this paper, including multinomial, normal, gamma, Poisson and binomial distributions.

Through the adoption of the projection theorem and divergence minimisation between prior or posterior conjugate and approximated specifications, the proposed method aligns, to some extent, with recent advances in variational inference (Blei et al., 2017), with the advantage of jointly addressing all the components of the latent states vector. An illustrative example relevant to our study is Koop and Korobilis (2023), which applies variational Bayes inference for the estimation of high-dimensional state-space models. Our proposed method ensures tractability, computational efficiency and online inference. Point estimates, predictions and joint uncertainty characterisation are comparable to those obtained via stochastic simulation methods. It compares favourably with methods that induce dynamics at a locally steady level (e.g., Smith, 1979; Harvey and Fernandes, 1989; Gamerman et al., 2013). Implementation of the proposed method is facilitated by the `kDGLM` package (dos Santos Jr. et al., 2024), which was developed along with this investigation and is available in CRAN-R.

One of our contributions is to present a real-time inferential procedure for dynamic multinomial models, effectively managing category dependencies while maintaining sequential analysis. Our adaptable framework can be extended to accommodate compositional

data and flexible predictor specifications. In this sense, our work aligns with the dynamic compositional models of Grunwald et al. (1993); Cargnoni et al. (1997); Terui et al. (2010); and Berry and West (2020).

The paper is structured as follows: the background and other inference techniques for DGLMs are discussed in Section 2; information geometry principles are introduced and the algorithmic development of our proposal is detailed in Section 3; and applications using artificial and classical time series data are shown in Section 4, with examples that include a multinomial dynamic model for synthetic data, normal and gamma dynamic models for stochastic volatility and a Poisson dynamic models for quarterly sales. A case study of age-grouped hospital admissions in Brazil is presented in Section 5. The paper concludes in Section 6 with some comments and suggestions for future work.

2 A Review of Dynamic Generalised Linear Models

In this section, we review key concepts, underlying the models used throughout this paper. We focus on time-indexed observables y_t , $t = 1, 2, \dots$, which follow a k -parametric exponential family distribution ($k \geq 1$) and are assumed to be conditionally independent given the k -dimensional parameter vector $\boldsymbol{\eta}_t$. The probability density (or mass) function of the observables is expressed as $p(y_t|\boldsymbol{\eta}_t) = f(y_t)a(\boldsymbol{\eta}_t) \exp\left\{\sum_{i=1}^k c_i\phi_i(\boldsymbol{\eta}_t)h_i(y_t)\right\}$, which can be rewritten in canonical form as:

$$p(y_t|\boldsymbol{\psi}_t) = c(y_t)\exp\{\mathbf{H}'(y_t)\boldsymbol{\psi}_t - b(\boldsymbol{\psi}_t)\}, \quad (1)$$

where $\mathbf{H}(y_t) = (h_1(y_t), \dots, h_k(y_t))'$ is a sufficient statistic vector matching the dimension of the parameter vector $\boldsymbol{\eta}_t$, and $\boldsymbol{\psi}_t$ is the canonical parameter at time t , given by $\boldsymbol{\psi}_t = (\psi_{1t}, \dots, \psi_{kt})'$ and $\psi_{it} = c_i\phi_i(\eta_t)$ for $i = 1, \dots, k$. Note that the parameter vector is k -dimensional, but y_t can be univariate or multivariate.

The conjugate prior distribution $CP(\tau_0, \boldsymbol{\tau})$ for $\boldsymbol{\psi}_t$ is expressed as $p(\boldsymbol{\psi}_t|\boldsymbol{\tau}) = [K(\tau_0, \boldsymbol{\tau})]^{-1} \exp[\boldsymbol{\tau}'\boldsymbol{\psi}_t - \tau_0b(\boldsymbol{\psi}_t)]$, where $\boldsymbol{\tau}' = (\tau_1, \dots, \tau_k)$.

It is well established that if $y_t|\psi_t$ follows a distribution in the exponential family, then $E[\mathbf{H}(y)] = \nabla b(\boldsymbol{\psi})$ and $V[\mathbf{H}(y)] = \nabla^2 b(\boldsymbol{\psi})$, where ∇ is the differential operator. For regular exponential families (Bernardo and Smith, 2009), and under conjugate priors, posterior and predictive distributions are analytically tractable, except when the normalising constant of the conjugate prior is unknown. Specifically, the posterior density of $\boldsymbol{\psi}_t$ given a new observation y_t at time t is $p(\boldsymbol{\psi}_t|y_t, \tau_0, \boldsymbol{\tau}) = p(\boldsymbol{\psi}_t|\tau_0^*, \boldsymbol{\tau}^*)$, where $\tau_0^* = \tau_0 + 1$ and $\boldsymbol{\tau}^* = \boldsymbol{\tau} + \mathbf{H}(y_t)$, with $\boldsymbol{\tau} + \mathbf{H}(y_t) = (\tau_1 + h_1(y_t), \dots, \tau_k + h_k(y_t))'$. The predictive distribution for a future observation y_f is given by $p(y_f|y_t, \tau_0, \boldsymbol{\tau}) = c(y_f)K(\tau_0^* + 1, \boldsymbol{\tau}^* + \mathbf{H}(y_f))/K(\tau_0^*, \boldsymbol{\tau}^*)$, where $\mathbf{H}(y_f) = (h_1(y_f), \dots, h_k(y_f))'$.

The DGLM class, introduced by West et al. (1985), is focused on uniparametric exponential families, establishing a connection between parameters $\boldsymbol{\eta}_t$ and a dynamic linear predictor $\mathbf{F}'_t \boldsymbol{\theta}_t$ via an invertible link function $\mathbf{g}(\cdot)$. A conjugate prior $\text{CP}(\tau_{0t}, \boldsymbol{\tau}_t)$ is assigned to the canonical parameter $\boldsymbol{\psi}_t = \mathbf{c}\boldsymbol{\phi}(\boldsymbol{\eta}_t)$ and the states $\boldsymbol{\theta}_t$ prior is partially specified, in terms of first and second moments. In the k -parametric exponential family extension, hereafter referred to as k DGLM, the model is defined by three components: an observable k -parametric exponential family model (see equation (1)); a relation linking $\boldsymbol{\eta}_t$ to a dynamic predictor vector $\boldsymbol{\lambda}_t$ governed by states $\boldsymbol{\theta}_t$ ($\mathbf{g}(\boldsymbol{\eta}_t) = \mathbf{F}'_t \boldsymbol{\theta}_t = \boldsymbol{\lambda}_t$); and an evolution equation for the latent states $\boldsymbol{\theta}_t = \mathbf{G}'_t \boldsymbol{\theta}_{t-1} + \boldsymbol{\omega}_t$ with $\boldsymbol{\omega}_t \sim N_p[\mathbf{0}, \mathbf{W}_t]$. Here, \mathbf{F}_t is a known $(p \times k)$ dynamic regression matrix, \mathbf{G}_t is a $(p \times p)$ state evolution matrix, \mathbf{W}_t is a $(p \times p)$ evolution covariance matrix, and \mathbf{g} is an invertible link function. The class provides conjugacy properties beneficial for sequential inference.

West et al. (1985) presented real-time inference in uniparametric exponential family DGLMs by partially specifying prior distributions for states $\boldsymbol{\theta}_t$ at each time step $t = 1, 2, \dots, T$, aligning moments of the conjugate prior with those from the partial state specification. New observations were seamlessly incorporated through Bayes' theorem, resulting in a closed-form posterior for the canonical parameter and analytically tractable predictive distributions. The dimensional imbalance between the p -dimensional state vector and the canonical parameter was resolved by employing linear Bayes estimation. Posterior

state moments transitioned into prior moments through the system equation, iterated up to time T and generating smoothed distributions for unobserved states using backward relations. Souza et al. (2016) introduced extended dynamic generalised linear models (EDGLMs) for the bivariate exponential family, building upon West et al. (1985). EDGLMs employ a bivariate link function to relate linear predictors, defined by states $\boldsymbol{\theta}_t$, to the canonical parameter vector $\boldsymbol{\eta}_t$. The sequential inference algorithm, based on conjugacy and linear Bayes estimation, encounters a challenge since the conjugate updating step can involve more conditions than unknowns. A solution inspired by the generalised method of moments (GMM) was put forth to deal with this potential drawback.

In our study, we directly manage arbitrary dimensions of the parametric vector, thus avoiding the additional step introduced by Souza et al. (2016). By leveraging normal theory and properties of conditional expectation, we resolve issues arising from unbalanced dimensions between the canonical parameter vector and the state vector. Additionally, by incorporating information geometry arguments, we extend the works of West et al. (1985) and Souza et al. (2016), offering a comprehensive formulation for sequential inference in k -parametric dynamic generalised linear models for $k \geq 1$.

3 Sequential Inference in k DGLMs

In this section, we propose a method for sequentially updating DGLMs using the k -parametric exponential family. We assume conditionally independent observations y_t for $t = 1, 2, \dots$, described by the observational model defined by equation (1). The k -dimensional vector of dynamic predictors, in turn, is defined by equation (2) and guided by latent states that evolve according to the system or evolution equation (3):

$$\mathbf{g}(\boldsymbol{\eta}_t) = \mathbf{F}_t' \boldsymbol{\theta}_t = \boldsymbol{\lambda}_t, \quad (2)$$

$$\boldsymbol{\theta}_t = \mathbf{G}_t' \boldsymbol{\theta}_{t-1} + \boldsymbol{\omega}_t, \quad \boldsymbol{\omega}_t \sim N_p(\mathbf{0}, \mathbf{W}_t), \quad (3)$$

with \mathbf{F}_t , \mathbf{G}_t and \mathbf{W}_t as defined in Section 2. Let D_0 represent the initial information set before any observation. The model incorporates a p -variate normal prior specification: $(\boldsymbol{\theta}_1|D_0) \sim N_p(\mathbf{a}_1, \mathbf{R}_1)$. Discount factors are applied to implicitly specify \mathbf{W}_t (see West and Harrison, 1997, Chap. 6). Our proposal, based on *information geometry* principles, is summarised in Subsection 3.1 and a detailed description of the sequential updating method is provided in Section 3.2.

3.1 Essentials of Information Geometry

In this section, we provide a concise overview of the key concepts underlying our proposed algorithm for inference in the k -parametric DGLM (k DGLM). The core result is the *projection theorem* (see Amari, 2016), which is applied to reconcile prior and posterior distributions derived from the state vector specification and the conjugate prior for the canonical parameters.

Let \mathcal{M} be a manifold of probability distributions, $\mathcal{M} = \{p(\boldsymbol{\eta}|\boldsymbol{\tau}), \boldsymbol{\tau} \in \mathbf{E} \subset \mathbb{R}^k\}$, where $p(\boldsymbol{\eta}|\boldsymbol{\tau})$ represents a probability density function and $\boldsymbol{\tau} \in \mathbf{E}$ serves as a coordinate system. Specifically, we focus on the manifold of the exponential family probability distributions, as defined in equation (1). For simplicity, we suppress temporal indices and assume $p(\boldsymbol{\eta}|\boldsymbol{\tau}) = c(\boldsymbol{\eta}) \exp[\mathbf{H}'(\boldsymbol{\eta})\boldsymbol{\psi} - b(\boldsymbol{\psi})]$. Here, $b(\boldsymbol{\psi})$ denotes a convex cumulant generating function, and we examine the divergence associated with $b(\boldsymbol{\psi})$ (Amari, 2016).

The Bregman divergence is defined as $D_b[\boldsymbol{\psi}; \boldsymbol{\psi}_0] = b(\boldsymbol{\psi}) - [b(\boldsymbol{\psi}_0) + \nabla b(\boldsymbol{\psi}_0)(\boldsymbol{\psi} - \boldsymbol{\psi}_0)]$. For the special case where $b(\boldsymbol{\psi})$ is the free energy convex function of the exponential family (Amari, 2016, p.13), it results in the Kullback-Leibler (KL) divergence between distributions p and q :

$$D_{KL}[p(\boldsymbol{\eta}|\boldsymbol{\tau}'); q(\boldsymbol{\eta}|\boldsymbol{\tau})] = \int p(\boldsymbol{\eta}|\boldsymbol{\tau}') \log \left(\frac{p(\boldsymbol{\eta}|\boldsymbol{\tau}')}{q(\boldsymbol{\eta}|\boldsymbol{\tau})} \right) d\boldsymbol{\eta}.$$

Our method to approximate priors and posteriors is a specific instance of Theorem 1.4 in Amari (2016).

Theorem 3.1 (*Projection theorem*) *Let $p(\boldsymbol{\eta})$ denote a probability distribution over a set*

\mathcal{Y} and let S represent an exponential family over \mathcal{Y} . The distribution $q(\boldsymbol{\eta})$ within S that minimises the Kullback-Leibler divergence $D_{KL}(p \parallel q)$ satisfies $E_q(\mathbf{H}_q) = E_p(\mathbf{H}_q)$, where \mathbf{H}_q denotes the vector of sufficient statistics under q and E_p, E_q , respectively, denote expectations under p and q .

The proof of Theorem 3.1 is straightforward.

3.2 Sequential learning in k DGLMs

The method of *conjugate updating* proposed by West et al. (1985), as briefly outlined in Section 2, characterises the probabilistic nature of states through their first and second moments. In contrast to restricting reconciliation to moment-based specifications, we propose reconciling entire prior or posterior densities. We argue that it is reasonable to measure discrepancies between density curves, since proximity in the parametric space may not accurately reflect closeness of prior or posterior specifications. In our proposal, we additionally assume a normal prior distribution for states $\boldsymbol{\theta}_t$ resulting in a k -dimensional Gaussian distribution for the linear predictors $\boldsymbol{\lambda}_t$. Our objective is to minimise the Kullback-Leibler divergence between this Gaussian prior and the joint conjugate prior for $\boldsymbol{\lambda}_t = \mathbf{g}(\boldsymbol{\eta}_t)$. Although this involves minimising divergence between two prior densities, the problem ultimately reduces to an optimisation task within the parametric space. At each time t , we aim to find the parameters $\boldsymbol{\tau}_t$ of the conjugate prior for $\boldsymbol{\eta}_t$ that minimise the KL divergence between the Gaussian prior and the conjugate prior.

Once the conjugate prior is fully specified and y_t is observed, updating is executed via Bayes' theorem. This yields a posterior distribution within the same parametric family as the prior, with updated parameters $\boldsymbol{\tau}_t^*$. Then we face another optimisation problem due to the asymmetry of the Kullback-Leibler divergence ($D_{KL}[p(y) : q(y)] \neq D_{KL}[q(y) : p(y)]$). Our objective, then, is to minimise the KL divergence between the posterior distribution of the linear predictors, as implied by the conjugate posterior, and a k -variate normal distribution for the same entity, $\boldsymbol{\lambda}_t$. Given that $\boldsymbol{\lambda}_t$ is a linear transformation of $\boldsymbol{\theta}_t$, and assuming prior normality of the states, $(\boldsymbol{\theta}_t, \boldsymbol{\lambda}_t | D_{t-1})$ follows a Gaussian distribution, where $D_{t-1} =$

$\{D_0, y_1, \dots, y_{t-1}\}$. Consequently, normal theory provides a closed-form analytical solution for the conditional distribution $(\boldsymbol{\theta}_t | \boldsymbol{\lambda}_t, D_{t-1})$. The distribution of $(\boldsymbol{\lambda}_t | D_t)$ is approximated using a normal specification, and the updated distribution of $\boldsymbol{\theta}_t$ depends on y_t only through $\boldsymbol{\lambda}_t$. Thus, the first and second moments of $(\boldsymbol{\theta}_t | D_t)$ are determined as in West and Harrison (1997, p.639). This posterior distribution at time t evolves to a prior specification for $\boldsymbol{\theta}_{t+1}$, and the learning cycle repeats.

Algorithm 1 outlines the information filtering process in our method. We use the notation established in West and Harrison (1997) for the mean vectors and covariance matrices:

i) posterior distribution at time $t - 1$: $\mathbf{m}_{t-1} = E[\boldsymbol{\theta}_{t-1} | D_{t-1}]$ and $\mathbf{C}_{t-1} = \text{Cov}[\boldsymbol{\theta}_{t-1} | D_{t-1}]$;

ii) prior distribution for time t : $\mathbf{a}_t = E[\boldsymbol{\theta}_t | D_{t-1}]$ and $\mathbf{R}_t = \text{Cov}[\boldsymbol{\theta}_t | D_{t-1}]$;

iii) one-step-ahead predictive distribution of the linear predictor: $\mathbf{f}_t = E[\boldsymbol{\lambda}_t | D_{t-1}]$ and $\mathbf{Q}_t = \text{Cov}[\boldsymbol{\lambda}_t | D_{t-1}]$;

iv) posterior distribution of the linear predictor at time t : $\mathbf{f}_t^* = E[\boldsymbol{\lambda}_t | D_t]$ and $\mathbf{Q}_t^* = \text{Cov}[\boldsymbol{\lambda}_t | D_t]$.

As shown in Algorithm 2, smoothed estimates of the posterior moments, $E[\boldsymbol{\theta}_{t-k} | D_t]$ and $\text{Cov}[\boldsymbol{\theta}_{t-k} | D_t]$, for $k = 1, \dots, t - 1$ are trivially obtained. After determining the posterior moments of the states and defining \mathbf{F}_{t+j} and \mathbf{G}_{t+j} , one can also obtain j -step-ahead distributions of $(\boldsymbol{\theta}_{t+j} | D_t)$ and predictive distributions. Algorithm 2 details the steps involved in smoothing and prediction.

Algorithm 1: Filtering and one-step ahead prediction in k DGLMs

Step 1: *Evolution.* Given \mathbf{m}_{t-1} , \mathbf{C}_{t-1} , and $\mathbf{F}'_t \boldsymbol{\theta}_t = \boldsymbol{\lambda}_t$, compute:

$$\begin{aligned} \mathbf{a}_t &= \mathbf{G}_t \mathbf{m}_{t-1}; & \mathbf{R}_t &= \mathbf{G}_t \mathbf{C}_{t-1} \mathbf{G}'_t + \mathbf{W}_t \\ \mathbf{f}_t &= \mathbf{F}'_t \mathbf{a}_t; & \mathbf{Q}_t &= \mathbf{F}'_t \mathbf{R}_t \mathbf{F}_t. \end{aligned}$$

Step 2: Given \mathbf{f}_t and \mathbf{Q}_t , determine the parameters $\boldsymbol{\tau}_t$ of the conjugate prior:

- *Step 2.1:* Compute the vector of sufficient statistics $\mathbf{H}_q(\boldsymbol{\eta}_t)$ for the conjugate distribution $q(\boldsymbol{\eta}_t | \boldsymbol{\tau}_t)$.
- *Step 2.2:* Obtain $\boldsymbol{\tau}_t$ such that $E_p(\mathbf{H}_q(\boldsymbol{\eta}_t)) = E_q(\mathbf{H}_q(\boldsymbol{\eta}_t))$, where the induced distribution is $p(\boldsymbol{\eta}_t | \mathbf{f}_t, \mathbf{Q}_t)$.

Step 3: Update the distribution of $\boldsymbol{\eta}_t$ using Bayes' theorem, obtaining: $\boldsymbol{\tau}_t^* = \boldsymbol{\tau}_t + \mathbf{h}(\mathbf{y}_t)$.

Step 4: Given $\boldsymbol{\tau}_t^*$, determine the updated parameters \mathbf{f}_t^* and \mathbf{Q}_t^* for the linear predictor:

- *Step 4.1:* Assuming that $q(\boldsymbol{\lambda}_t | \mathbf{f}_t^*, \mathbf{Q}_t^*)$ is a k -variate normal density, the vector of sufficient statistics is $\mathbf{H}_q(\boldsymbol{\lambda}_t) = [\boldsymbol{\lambda}_t, \boldsymbol{\lambda}_t \boldsymbol{\lambda}'_t]$.
- *Step 4.2:* Determine $(\mathbf{f}_t^*, \mathbf{Q}_t^*)$ such that $E_p(\mathbf{H}_q(\boldsymbol{\lambda}_t)) = E_q(\mathbf{H}_q(\boldsymbol{\lambda}_t))$, where the induced distribution is $p(\boldsymbol{\lambda}_t | \boldsymbol{\tau}_t^*) = p_{\boldsymbol{\eta}_t | \boldsymbol{\tau}_t^*}(\mathbf{g}(\boldsymbol{\eta}_t)) \left| \nabla_{\boldsymbol{\lambda}_t} \mathbf{g}(\boldsymbol{\eta}_t) \right|$.

Step 5: Obtain the posterior state moments:

$$\mathbf{m}_t = \mathbf{a}_t + \mathbf{R}_t \mathbf{F}_t \mathbf{Q}_t^{-1} (\mathbf{f}_t^* - \mathbf{f}_t); \quad \mathbf{C}_t = \mathbf{R}_t + \mathbf{R}_t \mathbf{F}_t \mathbf{Q}_t^{-1} (\mathbf{Q}_t^* - \mathbf{Q}_t) \mathbf{Q}_t^{-1} \mathbf{F}'_t \mathbf{R}_t.$$

Algorithm 2: Smoothing and J -steps-ahead forecast distributions

Step 1: Given \mathbf{a}_t , \mathbf{R}_t , \mathbf{m}_t , and \mathbf{C}_t , compute the smoothed posterior moments for $t = 1, \dots, T$:

$$\begin{aligned} \mathbf{m}_t^s &= \mathbf{m}_t + \mathbf{C}_t \mathbf{G}'_{t+1} \mathbf{R}_{t+1}^{-1} (\mathbf{m}_{t+1}^s - \mathbf{a}_{t+1}), \\ \mathbf{C}_t^s &= \mathbf{C}_t + \mathbf{C}_t \mathbf{G}'_{t+1} \mathbf{R}_{t+1}^{-1} (\mathbf{C}_{t+1}^s - \mathbf{R}_{t+1}) \mathbf{R}_{t+1}^{-1} \mathbf{G}_{t+1} \mathbf{C}_t. \end{aligned}$$

where $\mathbf{m}_T^s = \mathbf{m}_T$, $\mathbf{C}_T^s = \mathbf{C}_T$.

Step 2: Given \mathbf{m}_T , \mathbf{a}_T , \mathbf{R}_T , \mathbf{C}_T , \mathbf{F}_{t+j} , and \mathbf{G}_{t+j} , compute the j -steps-ahead prior for the linear predictor:

$$\mathbf{f}_t(j) = \mathbf{F}'_{t+j} \mathbf{a}_t(j); \quad \mathbf{Q}_t(j) = \mathbf{F}'_{t+j} \mathbf{R}_t(j) \mathbf{F}_{t+j}, \quad j = 1, \dots, J.$$

where $\mathbf{a}_t(j) = \mathbf{G}_{t+j} \mathbf{a}_t(j-1)$ and $\mathbf{R}_t(j) = \mathbf{G}_{t+j} \mathbf{R}_t(j-1) \mathbf{G}'_{t+j} + \mathbf{W}_{t+j}$, with $\mathbf{a}_t(0) = \mathbf{m}_T$ and $\mathbf{R}_t(0) = \mathbf{C}_T$.

In the following sections, we present applications based on synthetic and real data, outlining the primary elements involved in the analytical development of our proposal.

4 Applications to Synthetic and Empirical Data

In this section, we show that the proposed method is a scalable solution for online inference in k -parametric DGLMs, effectively capturing stochastic components such as seasonality and trends. The algebraic complexity involved in the analytical development of the steps in Algorithms 1 and 2, for different responses in the exponential family, can be avoided by using the R package `kDGLM` (dos Santos Jr. et al., 2024), available in CRAN-R. Section 4.1 provides details on the implementation of the proposed method for multinomial responses. Sequential updating for binary classification time series (a notable particular case of the multinomial structure) is detailed in Appendix A.1. Section 4.2 presents the normal and gamma dynamic models, simulating applications to financial returns in the context of stochastic volatility. The supplementary material, available at github.com/silvaneojunior/paper_kparam, provides an in-depth examination of the particular normal and gamma cases of our proposal, which involve approximations that deserve further discussion. A real dataset is used to illustrate the application of the method. In a first illustration, presented in Section 4.2.2, normal and gamma dynamic formulations are used to model monthly returns of IBM stocks. Additionally, in Section ?? of the supplementary material, a Poisson dynamic model is applied to a traditional quarterly sales time series, including stochastic trend and seasonal components. This illustration shows the advantages of our method over an alternative that depends on a locally constant level model, both in terms of modelling - allowing dynamic attributes to any latent components of the predictor -and computational efficiency.

In what follows, to streamline notation in the algorithmic development of the method for exponential family members, time indexes are occasionally omitted. However, all relations described in the following sections apply to each time t .

4.1 Multinomial model for synthetic data

In this section, we emphasise the k -parametric nature of the proposed method, which differentiates it from other sequential, cost-effective alternatives. Data were generated from a multinomial dynamic model with $k = 3$ categories. We validate the approximate inference produced by the proposed method by showing that the estimated posterior closely matches the true posterior obtained via NUTS in Stan (Carpenter et al., 2017).

The implementation of our sequential approach follows the algorithms outlined in Section 3.2. Let $y|\boldsymbol{\pi} \sim \text{Multinomial}(N, \boldsymbol{\pi})$, $\boldsymbol{\pi} = \boldsymbol{\eta} = (\pi_1, \pi_2, \dots, \pi_{d+1})$, where $0 < \pi_l < 1$, $\sum_{l=1}^d \pi_l \leq 1$, $\pi_{d+1} = 1 - \sum_{l=1}^d \pi_l$, $\sum_{l=1}^d y_l \leq N$, and $y_{d+1} = N - \sum_{l=1}^d y_l$. The conjugate prior is a Dirichlet density: $q(\boldsymbol{\pi}|\boldsymbol{\tau}) = \frac{1}{\prod_{l=1}^{d+1} \tau_l} \exp \left[\sum_{l=1}^d \tau_l \log \left(\frac{\pi_l}{\pi_{d+1}} \right) + \tau_0 \log \pi_{d+1} + \log B(\boldsymbol{\tau}) \right]$, with $B(\boldsymbol{\tau}) = \frac{\Gamma(\tau_0)}{\prod_{l=1}^{d+1} \Gamma(\tau_l)}$. Define the vector of linear predictors as $\boldsymbol{\lambda} = (\lambda_1, \dots, \lambda_d)' = \left[\log \left(\frac{\pi_1}{\pi_{d+1}} \right), \dots, \log \left(\frac{\pi_d}{\pi_{d+1}} \right) \right]' = \mathbf{F}'\boldsymbol{\theta}$ and assume that $\boldsymbol{\lambda} \sim N_d(\mathbf{f}, \mathbf{Q})$.

Following Algorithm 1, the sufficient statistics vector under the conjugate prior is:

$$\mathbf{H}_q(\boldsymbol{\pi}) = \left(\log \left(\frac{\pi_1}{\pi_{d+1}} \right), \dots, \log \left(\frac{\pi_d}{\pi_{d+1}} \right), \log(\pi_{d+1}) \right).$$

Thus, the system to be solved in Step 2.2 is $E_q[\mathbf{H}_q(\boldsymbol{\pi})] = E_p[\mathbf{H}_q(\boldsymbol{\pi})]$, where p is the prior density derived from the normal specification for the linear predictors. This system reduces to:

$$\begin{cases} \gamma(\tau_i) - \gamma \left(\sum_{l=1}^{d+1} \tau_l \right) & = f_i, \quad i = 1, \dots, d, \\ \gamma(\tau_{d+1}) - \gamma \left(\sum_{l=1}^{d+1} \tau_l \right) & \approx \log \left(\frac{1}{1 + \sum_{l=1}^d e^{f_l}} \right) + \frac{1}{2} \text{tr}(\tilde{\mathbf{H}}\mathbf{Q}), \end{cases}$$

where $\tilde{\mathbf{H}}$ is the Hessian of $f(\lambda_1, \dots, \lambda_d) = \log \left(\frac{1}{1 + \sum_{l=1}^d e^{\lambda_l}} \right)$, and $\gamma(\cdot)$ is the digamma function, which is approximated by:

$$\gamma(x) \approx \log(x) - \frac{1}{2x} - \frac{1}{12x^2}. \quad (4)$$

Step 3 updates the conjugate prior hyperparameters to $\tau_l^* = \tau_l + y_l$ for $l = 1, \dots, d$ and

$\tau_0^* = \tau_0 + N$. Now, let q be a multivariate normal density for the vector of linear predictors, with sufficient statistics vector $\mathbf{H}_q = (\boldsymbol{\lambda}, \boldsymbol{\lambda}\boldsymbol{\lambda}')'$. In Step 4.2, the system $E_q[\mathbf{H}_q(\boldsymbol{\lambda})] = E_p[\mathbf{H}_q(\boldsymbol{\lambda})]$ must be solved, where, now, p is the updated conjugate distribution. This reduces to: $f_l^* = \gamma(\tau_l^*) - \gamma(\tau_{d+1}^*)$ and $Q_{ll'}^* = \gamma'(\tau_l^*)I_{(l=l')} + \gamma'(\tau_{d+1}^*)$, where $\gamma'(\cdot)$ denotes the trigamma function and $I_{(l=l')}$ is the indicator function of $l = l'$.

Finally, the updated moments of the states $\boldsymbol{\theta}$ are obtained assuming a joint normal distribution for $\boldsymbol{\lambda}$ and $\boldsymbol{\theta}$ and using properties of the normal distribution to obtain the conditional distribution of $\boldsymbol{\theta}$ on $\boldsymbol{\lambda}$ (see West and Harrison, 1997, p. 639).

Predictions of future realizations of the observables are trivially obtained using the predictive Dirichlet-multinomial($N, \boldsymbol{\tau}$) density.

The efficiency of the method was evaluated for the updating of a dynamic multinomial model, through the generation of synthetic data from the model:

$$\begin{aligned} Y_1, Y_2, Y_3 | \boldsymbol{\eta}_t &\sim \text{Multinomial}(N, \boldsymbol{\eta}_t), \\ \log\left(\frac{\eta_{i,t}}{\eta_{3,t}}\right) &= \theta_{i,t}, i = 1, 2, \\ \theta_{i,t} &= \theta_{i,t} + \omega_{i,t}, \forall i, \end{aligned} \tag{5}$$

with $\omega_{1,t}, \omega_{2,t} \stackrel{\text{iid}}{\sim} \mathcal{N}(0, W_t)$, and $W_t = 0.01$. The number of categorical allocations for the response was set at $N = 1, 2, 5, 10, 20, 50, 100$. The frequentist properties of the inference produced by the proposed sequential approximation were evaluated by generating 500 data replicates for each N . Both our sequential approach and non sequential stochastic simulation through Stan were used to fit the model for each sample replicate.

Figure 1 presents a frequentist analysis of the bias in one-step-ahead predictions of $Y_{1,T+1}$ and $Y_{2,T+1}$, and in smoothed estimates of $\theta_{1,T}$ and $\theta_{2,T}$, for $T = 100$. This analysis is based on 500 synthetic data replicates and examines the accuracy of the proposed method under different specifications of the number N of categorical allocations in the multinomial design. Additional analyses for different sample sizes T , varying from $T = 2$ to $T = 50$, are presented in the supplementary material available at github.com/silvaneojunior/paper_kparam.

The results show that the sample T size has little impact on the approximation quality of our method. As for the number of categorical allocations N , the range of the bias across replicates approximates the ranges obtained via Stan N increases, with a significant reduction in the gap between methods for $N \geq 10$. As observed, for $N \geq 5$, the inference obtained through the proposed method is approximately equivalent to that derived using NUTS via Stan, for sample sizes varying from $T = 2$ to $T = 100$.

In Section 5, a multinomial dynamic model with trend and seasonal components is applied to real data in an epidemiological context to demonstrate the practical utility of the dynamic multinomial formulation, as well as the flexibility of the proposed method in accommodating structures with varying dynamic structural blocks for predictors in k -parametric models.

4.2 Stochastic volatility using normal and gamma kDGLMs

This section outlines the development of the suggested method for a distinguished univariate/biparametric member of the exponential family, handling both the mean and precision of normally distributed responses with dynamic predictors. To enhance the discussion, we provide examples within the framework of stochastic volatility, contrasting the Gaussian formulation with a more traditional method based on dynamic gamma models.

Financial decision making often relies on volatility as a risk indicator. The foundations of stochastic volatility (SV) models are strongly related to financial theories, and from a practical point of view, they are able to appropriately capture the main empirical properties of financial return series. A traditional return model is $y_t = e^{h_t/2}\epsilon_t$, $\epsilon_t \sim N(0, 1)$, or $\log(y_t^2) = h_t + a_t$, where h_t follows an AR(1) process with autoregressive coefficient γ and a_t follows a log- χ^2 distribution, usually approximated by a mixture of normals (Chib et al., 2009). We propose two dynamic approaches within the k -parametric exponential family. The first employs a normal model addressing the returns at their original scale, associating mean and precision with dynamic structures. The second uses a dynamic gamma model for the squared returns.

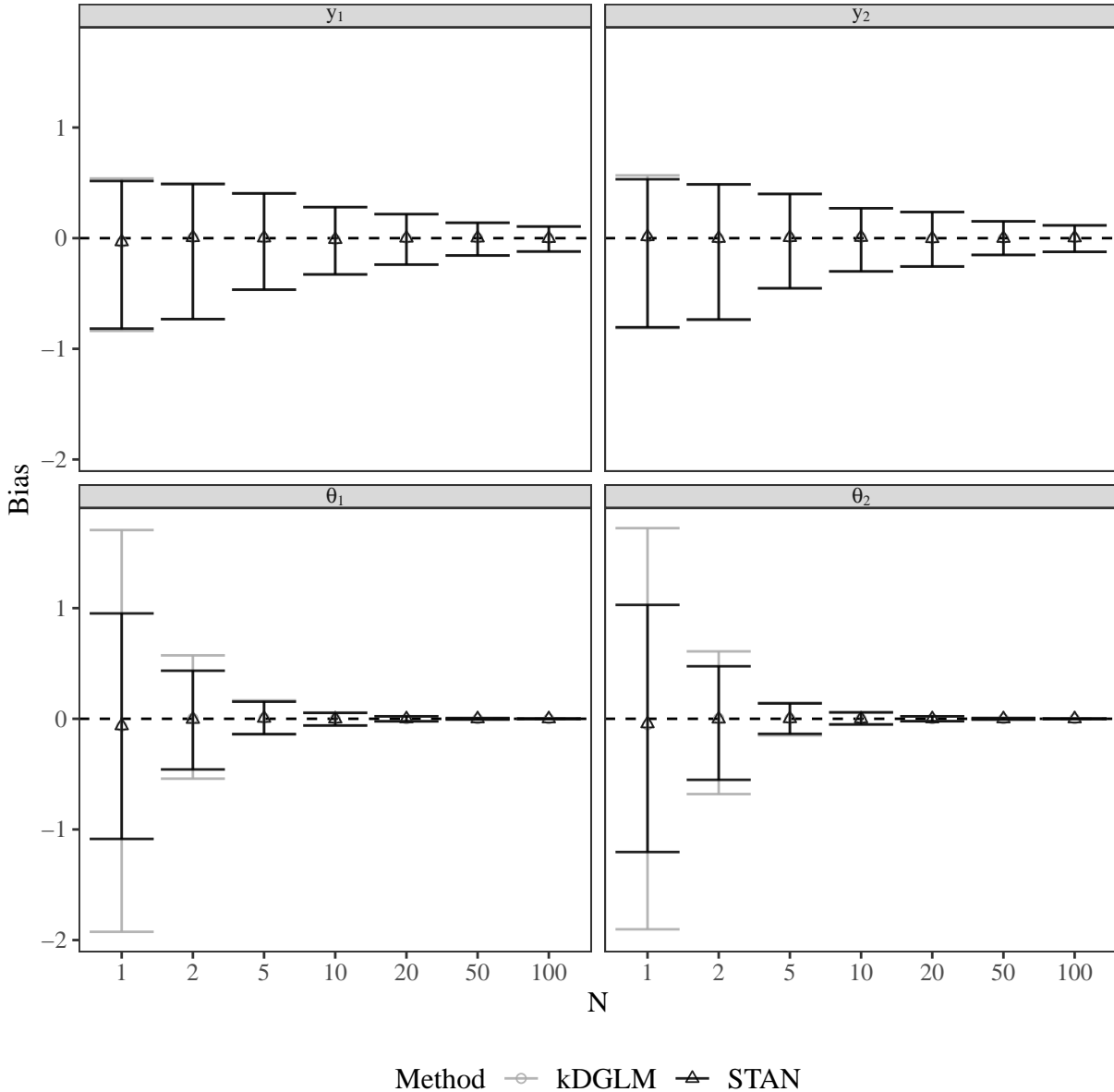


Figure 1: The bias of the one-step-ahead prediction of $Y_{1,T+1}$ and $Y_{2,T+1}$, for $T = 100$. Triangles represent the average bias across 500 sample replicates, while the error bars represent the 0.975 and 0.025 quantiles for the bias across the replicates. To facilitate visualization, the bias is divided by N . Gray: Sequential kdGLM. Black: NUTS via Stan.

Normal biparametric dynamic model for the returns

The implementation of our approach for univariate Gaussian responses, with dynamic predictive structure for the mean and log-precision, follows Algorithm 1 described in Section 3.2. The bidimensional parameter vector is denoted by $\boldsymbol{\eta} = (\mu, \phi)$ and $(y|\boldsymbol{\eta}) \sim N(\mu, \phi^{-1})$, $\mu \in \mathfrak{R}$, $\phi > 0$. The conjugate prior is a normal-gamma density, hi-

erarchically structured as: $\mu|\phi \sim N[\mu_0, (c_0\phi)^{-1}]$, $\phi \sim \mathcal{G}(n_0/2, d_0/2)$. Consider a vector of linear predictors: $\boldsymbol{\lambda}(\boldsymbol{\eta}) = (\lambda_1, \lambda_2)' = (\mu, \log(\phi))' = (F_1'\theta_1, F_2'\theta_2)'$ and the reparameterisation: $c_0 = -2\tau_1$, $\mu_0 = -\frac{\tau_2}{2\tau_1}$, $\frac{d_0}{2} = \frac{\tau_2^2}{4\tau_1} - \tau_3$ and $\frac{n_0}{2} = \tau_0 + 1/2$. We follow Algorithm 1, noting that the conjugate prior sufficient statistic vector is $\mathbf{H}_q(\boldsymbol{\eta}) = (\phi\mu^2, \phi\mu, \phi, \log \phi)'$. Then, the solution of the system in Step 2.2, $E_q[\mathbf{H}_q(\boldsymbol{\eta})] = E_p[\mathbf{H}_q(\boldsymbol{\eta})]$, is:

$$\begin{cases} \tau_0 &= \frac{1}{q_2} - \frac{1}{2}, & \tau_1 &= -[2q_1 \exp(f_2 + Q_2/2)]^{-1} \\ \tau_2 &= -2\tau_1(f_1 + Q_{12}), & \tau_3 &= (f_1 + q_{12})\tau_2 - [q_2 \exp(f_2 + Q_2/2)]^{-1}. \end{cases}$$

Once a new observation y is available, the conjugate prior hyperparameters are updated to $\boldsymbol{\tau}^* = (\tau_1^*, \tau_2^*, \tau_3^*, \tau_0^*) = (\tau_1 - 1/2, \tau_2 + y, \tau_3 - y^2/2, \tau_0 + 1/2)$. Now one must reconcile the posterior distribution for the linear predictors implied by the conjugate distribution for $\boldsymbol{\eta}$ with a multivariate normal. Let q denote a multivariate normal density for the vector of linear predictors, with sufficient statistic vector: $\mathbf{H}'_q = (\boldsymbol{\lambda}, \boldsymbol{\lambda}\boldsymbol{\lambda}')$. Step 4.2 reduces to solving the system $E_q[\mathbf{H}_q(\boldsymbol{\lambda})] = E_p[\mathbf{H}_q(\boldsymbol{\lambda})]$, where p is the updated distribution, resulting in:

$$\begin{cases} f_1^* &= \mu_0^* & f_2^* &= \gamma(n_0^*/2) - \log(d_0^*/2) \\ Q_1^* &= \frac{d_0^*}{c_0^* n_0^*} & Q_{12}^* &= 0 & Q_2^* &= \gamma'(n_0^*/2). \end{cases}$$

The updated moments of the states $\boldsymbol{\theta}$ are trivially obtained by applying normal distribution properties. The predictive distribution for y_t is a Student-t density with n_0 degrees of freedom, location parameter μ_0 and scale parameter $d_0/c_0 n_0$, which can be evaluated when step 2.2 is completed. In order to guarantee that the system in Step 4.2 has a solution, we imposed a restriction on the parameter space. Details can be found in the supplementary material at github.com/silvaneojunior/paper_kparam.

For the specific purpose of modelling returns, let $y_t \sim N((\mu_t, \phi_t^{-1})$ and assume the following predictive dynamic structure for the mean returns and their log-precision $\log(\phi_t) = -h_t$: $\boldsymbol{\lambda}_t = (\lambda_{1t}, \lambda_{2t})' = (\mu_t, -h_t)'$; $(\mu_t, h_t, \gamma_t)' = (\mu_{t-1}, \gamma_{t-1}h_{t-1}, \gamma_{t-1})' + (\omega_{1t}, \omega_{2t}, \omega_{3t})'$, where $\gamma_t = \gamma$ is an autoregressive coefficient estimated according to the ideas in West and Harrison (1997, Chapter 13) which are naturally accommodated in our approach assuming

$\omega_{3t} = 0$ with probability 1. In the applications exhibited in Subsections 4.2.1 and 4.2.2, we adopted a normal prior for $\tanh^{-1}\{\gamma_t\}$, constraining γ to the interval $(-1,1)$, so that h_t is a stationary process.

Gamma dynamic model for squared returns

Considering the traditional SV model, $\log(y_t^2) = h_t + a_t$, with $a_t \sim \log - \chi^2$, it follows that $y_t^2 \sim \mathcal{G}\left(\frac{1}{2}, \frac{1}{2} \exp(-h_t)\right)$. Thus, the particular gamma case of our approach can be applied to model y_t^2 , with shape parameter $\alpha_t = \alpha = \frac{1}{2}$ and $\mu_t = e^{h_t}$. Then $\lambda_t = \log(\mu_t) = h_t$, with evolution given by $h_t = \gamma h_{t-1} + \omega_t$, where γ is an autoregressive parameter estimated following West and Harrison (1997, Chapter 13).

Gamma dynamic models with known shape parameter α can be implemented by following Algorithm 1 described in Section 3.2. The conjugate prior for $\eta = \mu$ is an inverse-gamma density $q(\eta|\boldsymbol{\tau}) = \frac{1}{\eta} \exp[-\tau_0 \log(\eta) - \tau_1/\eta - b(\tau_0, \tau_1)]$, where $b(\tau_0, \tau_1) = \log(\Gamma(\tau_0)) - \tau_0 \log(\tau_1)$. Consider the linear predictor: $\lambda = \log(\mu) = \mathbf{F}'\boldsymbol{\theta}$ and the conjugate prior sufficient statistic vector: $\mathbf{H}'_q(\eta) = (-\log(\eta), -1/\eta)$. Following Algorithm 1 and using the fact that $E_q[\mathbf{H}_q(\eta)] = \nabla b(\tau_0, \tau_1)$ as well as approximation (4) for the digamma function, the solution of the system $E_q[\mathbf{H}_q(\eta)] = E_p[\mathbf{H}_q(\eta)]$ in Step 2.2 results in $\tau_1 = \tau_0 \exp(f - Q/2)$ and $\tau_0 = (1 + \sqrt{1 + 2Q/3})/(2Q)$. The conjugate prior hyperparameters are updated to $\tau_1^* = \tau_1 + y$ and $\tau_0^* = \tau_0 + \alpha$. Step 4.2 is completed by solving the system $E_q[\mathbf{H}_q(\boldsymbol{\lambda})] = E_p[\mathbf{H}_q(\boldsymbol{\lambda})]$, where, now, p is the updated conjugate distribution and q denotes a normal density for the linear predictor, with sufficient statistic vector: $\mathbf{H}'_q = (\lambda, \lambda^2)$. The following systems are generated: $f^* = \log(\tau_1^*) - \gamma(\tau_0^*)$ and $Q^* = \gamma'(\tau_0^*)$.

The predictive density for y_t is an inverse beta distribution (Aitchison and Dunsmore, 1975) with shape parameters τ_0 and α and scale parameter τ_1 , which can be evaluated once step 2.2 is completed. Note that from a probabilistic standpoint, the gamma and normal specifications for the volatility are equivalent, since if $y_t \sim N(0, e^{h_t})$, it follows that $y_t^2 \sim \mathcal{G}\left(1/2, e^{-h_t}/2\right)$, but, as previously mentioned, the normal formulation preserves the signals of the returns.

In Section 4.2.1, the proposed models and inferential approach are applied to artificial data, aiming to evaluate the performance of the normal and gamma dynamic formulations in capturing the volatility structure, as well as to compare the performance of our proposal to the results obtained via NUTS in Stan (Carpenter et al., 2017). The gamma and normal formulations based on our sequential method are then applied to a real dataset, as shown in Section 4.2.2

The development of the method for gamma observational models with an unknown shape parameter poses challenges due to the unknown normalising constant of the conjugate prior density of the pair (α, μ) . A detailed description of the proposed solution for updating dynamic gamma models with unknown shape α is presented in the supplementary material available at github.com/silvaneojunior/paper_kparam.

4.2.1 Modelling and estimation of volatilities: an illustration based on synthetic data

We simulated a time series of 365 observations, based on a dynamic normal structure, in order to evaluate the effectiveness of our method in recovering latent components of a stochastic volatility model. In order to perform a direct comparison of our approach with NUTS via Stan using identical models, we applied the normal formulation with a known evolution variance $Var(\omega_{2t})$ for the state h_t .

As shown in panel (A) of Figure 2, the volatility estimations under our sequential updating method for the normal and gamma models were nearly identical, as anticipated due to their equivalence. The proposed approach effectively captures volatility fluctuations, although a few time periods show exceptions. Figure 2, panel (B), exhibits the comparison of our sequential updating method for the normal dynamic model with non-sequential NUTS via Stan. For this specific model, the sequential implementation of the kDGLM method employs a linear approximation due to the unknown autoregressive coefficient γ in the evolution matrix \mathbf{G} . This approximation largely accounts for the discrepancies observed between the results of the proposed method and those obtained using NUTS in

Stan. Posterior summaries for the autoregressive coefficient γ are presented in Table 1. The sequential updates of the normal and gamma models produced nearly identical estimates, closely matching those from the Stan fit for the normal formulation. The true value $\gamma = 0.95$ was covered by the 95% credibility intervals across all scenarios. Stan required 15.4975 seconds—over 50 times longer than our method’s 0.187 seconds. The computational time of our approach scales linearly with the length of the time series, ensuring efficiency for long series. All computational times reported in this paper were measured with an i7-9750H CPU with 24 GB of RAM.

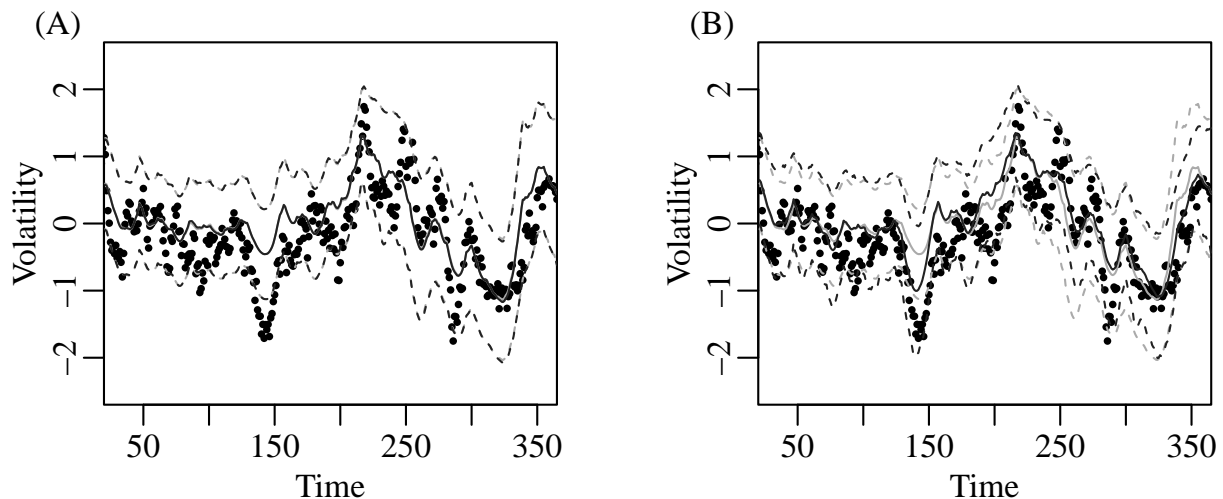


Figure 2: Comparison of smoothed means (solid lines) and credible intervals (dashed lines) for volatility estimation from synthetic data. The solid circles indicate theoretical volatilities. (A): results of the proposed sequential approach for normal (grey) and gamma (black) formulations. (B): comparison of normal formulation using the sequential approach (grey) and NUTS via Stan (black).

Model/ Inferential approach	Mean	2.5% quantile	97.5% quantile
Gamma/ kDGLM	0.934	0.898	0.971
Normal/ kDGLM	0.934	0.897	0.971
Normal/ NUTS	0.933	0.878	0.974

Table 1: Posterior summaries for the autoregressive coefficient (γ) in the normal and gamma stochastic volatility models for synthetic data, via sequential updating and NUTS via Stan.

Figure ?? in the supplementary material exhibits the inference results under kDGLM and NUTS, fixing parameter γ at its true value. As shown, the two methods yield nearly

identical results. Therefore, for models where the evolution matrix \mathbf{G} is known, the kDGLM method is expected to produce inferences closely aligned with those generated by Markov Chain Monte Carlo schemes. On the other hand, for long time series analysed using models where \mathbf{G} depends on hyper parameters that introduce non linearities in the system, and in contexts demanding real-time inference, a slight loss in accuracy or precision can be outweighed by the substantial computational efficiency offered by the kDGLM method.

4.2.2 Modelling and estimation of volatilities: an application to monthly IBM returns

This section presents the results of our proposed method, using normal and gamma dynamic formulations, to fit and forecast monthly IBM returns from January 1926 to December 1999. Data come from Tsay (2010).

The posterior summaries of the autoregressive coefficient γ are presented in Table 2. Similar to the synthetic data results, the normal and gamma formulations using the proposed sequential approach are nearly indistinguishable. These posterior summaries align with those obtained via NUTS in Stan.

Model/ Inferential approach	Mean	2.5% quantile	97.5% quantile
Gamma/ kDGLM	0.934	0.916	0.951
Normal/ kDGLM	0.933	0.915	0.951
Normal/ NUTS	0.938	0.906	0.965

Table 2: Posterior summaries of the autoregressive coefficient (γ) in the normal and gamma stochastic volatility models for the IBM return data, via sequential updating and Hamiltonian Monte Carlo - Stan.

Figure 3 displays the smoothed estimates for volatilities h_t . The normal and gamma formulations yield almost identical point estimates and credible intervals, as shown in panel (A). To objectively compare models, we calculated a Bayes factor; the normal model was superior. Indeed the predictive log-likelihood difference between models favoured the normal model by 316.3. As shown in panel (B), the sequential estimates for volatilities using both sequential updating and Stan are consistent, indicating that the proposed method provides

adequate approximations with significantly reduced computational time compared to a “gold standard” method that ensures convergence to the true posterior. Notably, sequential updating methods allow for the incorporation of external information at any time, which can be advantageous in econometric applications.

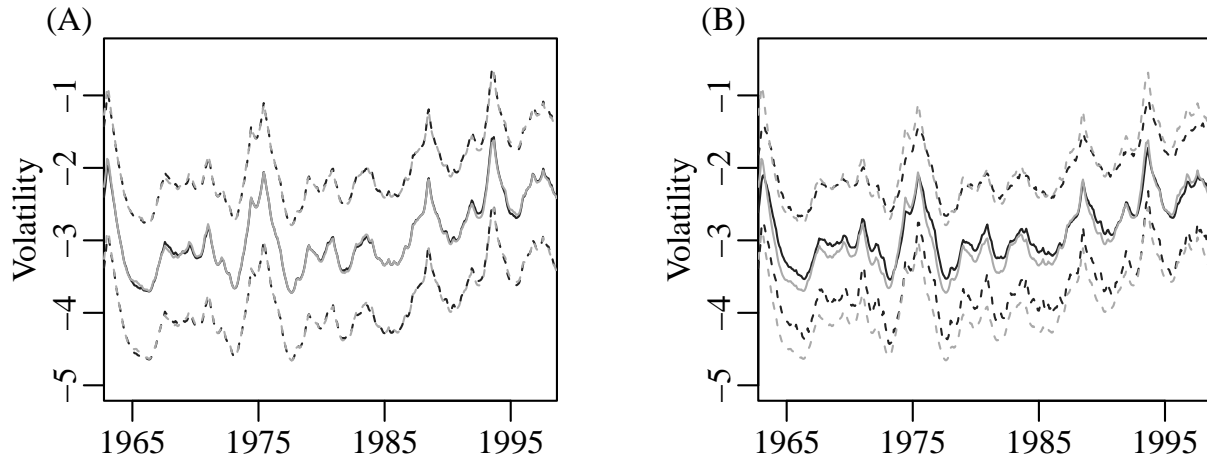


Figure 3: Smoothed mean and credibility intervals for IBM volatilities h_t . (A): Comparison between normal and gamma formulations using sequential kDGLM. (B): Sequential kDGLM estimates compared to Hamiltonian Monte Carlo estimates obtained via Stan.

A similar application was proposed by Souza et al. (2016), who used the generalised method of moments (GMM) to handle a system with more equations than parameters, but this introduced additional approximations and processing overhead. Our approach avoids these issues.

In the next section, we present an application of the proposed method to real data, considering a multivariate and multiparametric context.

5 An illustrative case study

Acute diarrheal disease, exacerbated by poor living conditions and malnutrition, poses a significant health threat in Brazil. Current monitoring focuses on non-cholera bacterial, viral, and parasitic outbreaks spread through food, water, and interpersonal contact. Dynamic Bayesian models facilitate monitoring epidemiological trends, also accommodating structural

shifts, predicting outbreaks, and quantifying intervention impacts.

Rotavirus is a major etiological agent of diarrhoeal disease, causing a substantial proportion of severe cases, hospitalisations, and deaths in Brazil (Ambrosini and Carraro, 2012). Since March 2006, the Rotarix[®] vaccine made by GlaxoSmithKline has been administered to children, significantly reducing hospitalisations and deaths in vaccinated age groups (Linhares and Justino, 2013). Ambrosini and Carraro (2012) reported substantial reductions in diarrhoea-related hospitalization rates in children up to age five after vaccination.

We analyse monthly hospital admission data for diarrhoea and gastroenteritis, in Brazil, from 2000 to 2022, using a dynamic multinomial model. This model captures age-specific patterns and assesses the contributions of different age groups to the pool of hospital admissions, particularly infants (<1 year) and young children (1-4 years), the age groups targeted by the rotavirus vaccine. The data are available at <http://tabnet.datasus.gov.br/>.

5.1 A multinomial model for hospital admissions

A preliminary cluster analysis of hospital admissions due to diarrhoea and gastroenteritis was applied, to detect correlations among time series across different age groups. Our main focus is on hospital admissions for infants, and the cluster analysis resulted in the following age groups: infants (<1 year); young children (1-4 years); children (5-14 years); youths/adults (15-59 years - reference group); and ≥ 60 years (seniors). Time series for the first two groups are exhibited as solid circles in Figure 4.

A dynamic multinomial model was fitted to the categorised data. Let $\mathbf{Y}_t = (Y_{1t}, \dots, Y_{5t})$, where Y_{jt} denotes the number of hospital admissions for age group $j = 1, 2, \dots, 5$. Assume that $\mathbf{Y}_t | \eta_{1t}, \eta_{2t}, \eta_{3t}, \eta_{4t}, \eta_{5t} \sim \text{Multinomial}(\eta_{jt}, j = 1 : 5)$ where $\eta_{5t} = \left(1 - \sum_{j=1}^4 \eta_{jt}\right)$ with predictive structure: $\lambda_{jt} = \log\left(\frac{\eta_{jt}}{\eta_{5t}}\right) = F'_{jt}\theta_{jt}$, $j = 1, 2, 3, 4$. The same dynamic structure, which was considered flexible enough to capture observed patterns in the real data, was adopted for each category: $F'_{jt} = [1, 0, 1, 0, 1]$; $G_{jt} = \text{blockdiag}[G_{trend}, G_{seasonal}, G_{noise}]$, $j = 1, \dots, 4$, where: $G_{trend} = \begin{bmatrix} 1 & 1 \\ 0 & 1 \end{bmatrix}$; $G_{seasonal} = \begin{bmatrix} \cos(\omega) & \sin(\omega) \\ -\sin(\omega) & \cos(\omega) \end{bmatrix}$, $\omega = \frac{2\pi}{12}$, $G_{noise} = 0$.

Therefore, $F'_t = \text{blockdiag}[F'_{1t}, F'_{2t}, F'_{3t}, F'_{4t}]$ and $G_t = \text{blockdiag}[G_{1t}, G_{2t}, G_{3t}, G_{4t}]$. Discount factors 0.95 and 0.975 were assigned for trend and seasonality, respectively. A noise component with variance 0.005 was included to accommodate overdispersion.

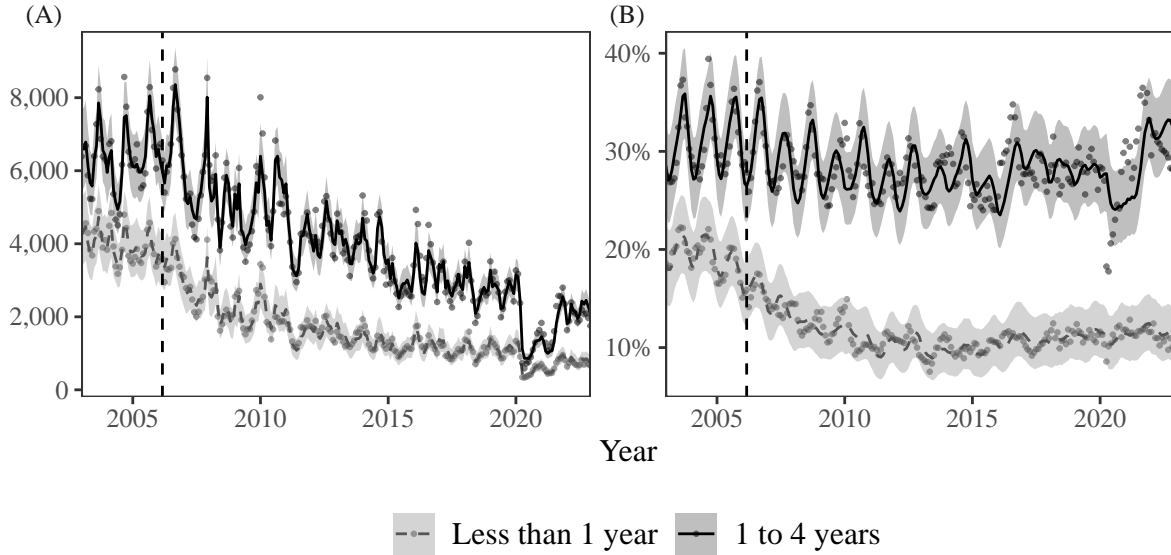


Figure 4: Observed values (solid circles) compared with one-step-ahead predictions for age groups 1 and 2: number of admissions (A); probability of hospital admission for each age group (B). The vertical dashed line indicates the moment of vaccine introduction.

The multinomial dynamic model provided estimates of compositional probabilities for different age groups, conditional on hospitalisation due to diarrhoeal disease or gastroenteritis. Sequential updating was carried out following the proposed kDGLM procedure detailed in Section 4.1. Using data from the Brazilian Institute of Geography and Statistics (IBGE) and Datasus, we estimated hospital admission probabilities conditionally on each age group (see Appendix A.3 for details).

Figure 4 demonstrates that our findings are consistent with the Brazilian epidemiological literature, showing a marked decline in hospital admission counts (Panel A) and probabilities (Panel B) for infants following the introduction of the rotavirus vaccine in the National Immunisation Plan. A similar decline is observed in admission counts and probabilities for the 1–4 year age group. Supplementary material, available at github.com/silvaneojunior/paper_kparam, includes interactive graphs presenting predictive results for all age groups.

A reduction in the probability of hospitalisation due to diarrhoea and gastroenteritis is evident across all age groups after vaccine introduction, with immediate effects for infants and gradual declines for older groups. This scaling effect likely reflects reduced rotavirus transmission and the progression of immunised individuals into subsequent age groups. The model also accounts for structural changes, such as the Covid-19 pandemic, capturing a sharp decline in hospital admissions during lockdowns and adapting to evolving patterns as restrictions were eased.

6 Concluding remarks and future research

In this study, we introduced a method for sequentially updating information in *dynamic generalised linear models* for univariate and multivariate responses within the k -parametric exponential family. The proposed method maintains key aspects of time series analysis, such as monitoring and intervention capabilities, and offers filtered and smoothed distributions, as well as forecasts, with minimal computational effort. This makes it a viable option for real-time analysis and timely decision making.

We detail the method for specific cases: multinomial (multivariate, k -parametric); Bernoulli and Poisson (univariate, uniparametric); gamma with dynamic linear predictors for mean and shape parameters (univariate, biparametric); and normal with dynamic linear predictors for mean and precision (univariate, biparametric).

The method builds on the conjugation properties of the exponential family and the Projection Theorem, reconciling conjugate prior and posterior distributions for canonical parameters with distributions induced by normality assumptions for the states that drive linear predictors. These predictors can accommodate stochastic trends, seasonality, and dynamic covariate effects.

We are expanding this method to other distributions, including Dirichlet compositional responses and multivariate normal outputs, focusing on multivariate stochastic volatility models. The `kDGLM` R package has been developed to implement the described models,

providing users with a tool for efficient dynamic modelling of both univariate and multivariate responses. kDGLM is available in CRAN-R and features automatic monitoring, intervention, autoregressive components, and transfer functions.

Acknowledgements

We thank Professor Heudson Mirandola (UFRJ), for his fruitful collaboration and suggestions, and Professor Alexandra Schmidt (McGill University) for her careful review of a preliminary version of this manuscript and valuable comments.

Funding

The research presented in this paper was partially supported by Fapesp grant 2019/00787-7, PAPD/UERJ, grant E-26/007/10667/2019 (H. S. Migon), and a CAPES grant (S.V. dos Santos Jr. and R. Marotta).

A Appendix

A.1 Analytical development of the proposed method for Bernoulli responses

Let $\eta = \pi$ and $y|\pi \sim Ber(\pi)$, $0 < \pi < 1$. $\psi(\pi) = \log(\frac{\pi}{1-\pi})$. The conjugate prior is a beta density $q(\pi|\boldsymbol{\tau}) = exp\{\tau_1 \log(\frac{\pi}{1-\pi}) + \tau_0 \log(1-\pi) - [\log(\Gamma(\tau_1 + 1)) + \log(\Gamma(\tau_0 - \tau_1 + 1)) - \log(\Gamma(\tau_0 + 2))]\}$, where $b(\tau_0, \tau_1) = [\log(\Gamma(\tau_1 + 1)) + \log(\Gamma(\tau_0 - \tau_1 + 1)) - \log(\Gamma(\tau_0 + 2))]$. Consider the linear predictor $\lambda = logit(\pi) = \mathbf{F}'\boldsymbol{\theta}$. Following Algorithm 1 :

- Step 1: Given posterior moments for the states, obtain the prior moments of $\lambda \sim N(f, Q)$.
- Step 2.1: Obtain the conjugate prior sufficient statistics vector: $\mathbf{H}'_q(\pi) = (\log(\frac{\pi}{1-\pi}), \log(1-\pi))$.

- Step 2.2: Using the fact that $E_q[\mathbf{H}(\pi)] = \nabla b(\tau_0, \tau_1)$, solve the system $E_q[\mathbf{H}_q(\pi)] = E_p[\mathbf{H}_q(\pi)]$, where p is the prior density induced by the normal specification for the linear predictors:

$$\begin{cases} \gamma(\tau_1 + 1) - \gamma(\tau_0 - \tau_1 + 1) = f \\ \gamma(\tau_0 - \tau_1 + 1) - \gamma(\tau_0 + 2) \simeq \log\left(\frac{1}{1+e^f}\right) - \frac{Qe^f}{(1+e^f)^2}. \end{cases}$$

A second-order Taylor approximation was applied and the system was solved using the Newton-Raphson method, with negligible computational cost.

- Step 3: Update the hyperparameters of the conjugate specification: $\tau_1^* = \tau_1 + y$, $\tau_0^* = \tau_0 + 1$.
- Step 4.1: Let q denote a normal density for the linear predictor, with sufficient statistics vector: $\mathbf{H}'_q = (\lambda, \lambda^2)$.
- Step 4.2: Solve the system $E_q[\mathbf{H}_q(\boldsymbol{\lambda})] = E_p[\mathbf{H}_q(\boldsymbol{\lambda})]$, where p is the updated distribution, obtaining: $f^* \simeq \gamma(\tau_1^* + 1) - \gamma(\tau_0^* - \tau_1^* + 1)$ and $Q^* = \gamma'(\tau_1^* + 1) + \gamma(\tau_0^* - \tau_1^* + 1)$.
- Step 5: The updated moments of the states $\boldsymbol{\theta}$ are trivially obtained, applying normal distribution properties.

The predictive distribution for y_t is a binomial-beta($\tau_0, \tau_1, 1$), which can be evaluated once step 2.2 is completed.

A.2 Multinomial model: obtaining the probabilities of hospital admission for each age group.

As seen in Subsection 5.1, for a multinomial response on k categories where the k -th category is used as a reference group, the following predictive structure is specified:

$$\lambda_{jt} = \log\left(\frac{\eta_{jt}}{\eta_{k,,t}}\right) = \mathbf{F}'_{jt}\boldsymbol{\theta}_t, \quad j = 1, \dots, k-1.$$

Let E_{jt} denote the exposure of group j ; $E_{1:k,t} = \sum_{j=1}^k E_{jt}$ denote the total exposure of all age groups, and consider the following events:

G_{jt} : allocation of an individual to age group j , $j = 1, \dots, k-1$; at time t , $t=1, 2, \dots$;

H_t : hospital admission of an individual at time t , $t=1, 2, \dots$

Note that the probability of allocation to age group j and time t , conditionally on having been hospitalized, is:

$$\eta_{jt} = \mathbb{P}(G_{jt}|H_t) = \frac{\mathbb{P}(H_t|G_{jt})\mathbb{P}(G_{jt})}{\mathbb{P}(H_t)} \Rightarrow \frac{\mathbb{P}(H_t|G_{jt})}{\mathbb{P}(H_t|G_{kt})} = \frac{\mathbb{P}(G_{jt}|H_t)}{\mathbb{P}(G_{kt}|H_t)} \frac{E_{kt}}{E_{jt}}.$$

Then it follows that:

$$\begin{aligned} \log \left\{ \frac{\mathbb{P}(H_t|G_{jt})}{\mathbb{P}(H_t|G_{kt})} \right\} &= \log \left\{ \frac{\mathbb{P}(G_{jt}|H_t)}{\mathbb{P}(G_{kt}|H_t)} \right\} - \log \left\{ \frac{E_{jt}}{E_{kt}} \right\} \\ &= \mathbf{F}'_{jt} \boldsymbol{\theta}_t - \log \left\{ \frac{E_{jt}}{E_{kt}} \right\}, \quad j = 1, \dots, k-1. \end{aligned}$$

Thus, estimates of $\mathbb{P}(H_t|G_{jt})$ are naturally obtained if $\log \left\{ \frac{E_{jt}}{E_{kt}} \right\}$ is introduced as an offset term in the dynamic predictor of category j , $j = 1, \dots, k-1$.

References

- Aitchison, J. and Dunsmore, I. (1975). Statistical Prediction Analysis. Cambridge University Press.
- Alves, M. B., Gamerman, D., and Ferreira, M. A. R. (2010). Transfer functions in dynamic generalized linear models. Statistical Modelling, 10:03 – 40.
- Amari, S. (2016). Information Geometry and its Applications. Springer.
- Ambrosini, V. A. and Carraro, E. (2012). *Impacto da vacinação de rotavírus no Brasil*. Revista Medicina Ribeirão Preto (Methodological Revision), 45(4):411–18.
- Bernardo, J. M. and Smith, A. F. (2009). Bayesian Theory, volume 405. John Wiley & Sons.
- Berry, L. R. and West, M. (2020). Bayesian forecasting of many count-valued time series. Journal of Business & Economic Statistics, 38(4):872–887.

- Blei, D. M., Kucukelbir, A., and McAuliffe, J. D. (2017). Variational inference: A review for statisticians. *Journal of the American Statistical Association*, 112(518):859–877.
- Cargnoni, C., Müller, P., and West, M. (1997). Bayesian forecasting of multinomial time series through conditionally Gaussian dynamic models. *Journal of the American Statistical Association*, 92(438):640–647.
- Carpenter, B., Gelman, A., Hoffman, M. D., Lee, D., Goodrich, B., Betancourt, M., Brubaker, M., Guo, J., Li, P., and Riddell, A. (2017). Stan: A probabilistic programming language. *Journal of Statistical Software*, 76(1):1–32.
- Carter, C. K. and Kohn, R. (1994). On Gibbs sampling for state space models. *Biometrika*, 81(3):541–553.
- Chib, S., Omori, Y., and Asai, M. (2009). Multivariate stochastic volatility. In Mikosch, T., Kreiß, J.-P., Davis, R. A., and Andersen, T. G., editors, *Handbook of Financial Time Series*, pages 365–400. Springer Berlin Heidelberg, Berlin, Heidelberg.
- da Silva, C. Q., Migon, H. S., and Correia, L. T. (2011). Dynamic Bayesian beta models. *Computational Statistics and Data Analysis*, 55(6):2074–89.
- dos Santos Jr., S. V., Alves, M. B., and Migon, H. S. (2024). *kDGLM: an R package for Bayesian analysis of generalized dynamic linear models*.
- Durbin, J. and Koopman, S. J. (2002). A simple and efficient simulation smoother for state space time series analysis. *Biometrika*, 89(3):603–15.
- Frühwirth-Schnatter, S. (1994). Data augmentation and dynamic linear models. *Journal of Time Series Analysis*, 15(2):183–202.
- Gamerman, D. (1998). Markov chain Monte Carlo for dynamic generalised linear models. *Biometrika*, 85(1):215–227.

- Gamerman, D., dos Santos, T. R., and Franco, G. C. (2013). A non-Gaussian family of state-space models with exact marginal likelihood. *Journal of Time Series Analysis*, 34(6):625–645.
- Grunwald, G. K., Raftery, A. E., and Guttorp, P. (1993). Time series of continuous proportions. *Journal of the Royal Statistical Society: Series B (Methodological)*, 55(1):103–116.
- Harrison, P. J. and Stevens, C. F. (1976). Bayesian forecasting. *Journal of the Royal Statistical Society. Series B (Methodological)*, 38(3):205–247.
- Harvey, A. C. and Fernandes, C. (1989). Time series models for count or qualitative observations. *Journal of Business & Economic Statistics*, 7(4):407–417.
- Koop, G. and Korobilis, D. (2023). Bayesian dynamic variable selection in high dimensions. *International Economic Review*, 64(3):1047–1074.
- Linhares, A. C. and Justino, C. A. (2013). Rotavirus vaccination in brazil: effectiveness and health impact seven years post-introduction. *Expert Rev Vaccines*, 13(1):43–57.
- Marotta, R. (2018). Revisiting dynamic linear models for p-dimensional exponential family. Master’s thesis, Universidade Federal do Rio de Janeiro, RJ BR.
- Migon, H., Gamerman, D., Lopes, H., and Ferreira, M. (2005). Dynamic models. In Dey, D. and Rao, C., editors, *Bayesian Thinking Modeling and Computation, Handbook of Statistics*, pages 553–588. Elsevier B.V.
- Migon, H. S., Alves, M. B., Menezes, A. F. B., and Pinheiro, E. G. (2023). A review of Bayesian dynamic forecasting models: Applications in marketing. *Applied Stochastic Models in Business and Industry*, 39(3):471–493.
- Migon, H. S., Schmidt, A. M., Ravines, R. E. R., and Pereira, J. B. M. (2013). An efficient sampling scheme for dynamic generalized models. *Computational Statistics*, 28:2267 – 2293.

- Nelder, J. A. and Wedderburn, R. W. M. (1972). *Generalized linear models*. Journal of the Royal Statistical Society, Series A, General, 135:370–384.
- Shephard, N. and Pitt, M. K. (1997). *Likelihood analysis of non-Gaussian measurement time series*. Biometrika, 84(3):653–67.
- Smith, J. (1979). *A generalization of the Bayesian steady forecasting model*. Journal of the Royal Statistical Society. Series B (Methodological), 41:375–387.
- Souza, M. A. O., Migon, H. S., and Pereira, J. (2016). *Extended dynamic generalized linear models: The two-parameter exponential family*. Computational Statistics & Data Analysis, 121:164–179.
- Terui, N., Ban, M., and Maki, T. (2010). *Finding market structure by sales count dynamics—Multivariate structural time series models with hierarchical structure for count data*. Annals of the Institute of Statistical Mathematics, 62(1):91–107.
- Tsay, R. S. (2010). Analysis of Financial Time Series. John Wiley & Sons, 3rd edition.
- West, M. and Harrison, P. J. (1997). Bayesian Forecasting and Dynamic Models. Springer, New York, NY.
- West, M., Harrison, P. J., and Migon, H. S. (1985). *Dynamic generalized linear models and Bayesian forecasting*. Journal of the American Statistical Association, 80(389):73–83.

Supplementary Material for: An Efficient Sequential Approach for k -parametric Dynamic Generalised Linear Models

Mariane B. Alves*, Helio S. Migon*, Silvano V. dos Santos Jr.*, Raíra Marotta*

*Instituto de Matemática, Universidade Federal do Rio de Janeiro, Rio de Janeiro, Brazil.

January 15, 2025

Abstract

A novel sequential inferential method for Bayesian dynamic generalised linear models is presented, addressing both univariate and multivariate k -parametric exponential families. It efficiently handles diverse responses, including multinomial, gamma, normal, and Poisson distributed outcomes, by leveraging the conjugate and predictive structure of the exponential family. The approach integrates information geometry concepts, such as the projection theorem and Kullback-Leibler divergence, and aligns with recent advances in variational inference. Applications to both synthetic and real datasets highlight its computational efficiency and scalability, surpassing alternative methods. The approach supports the strategic integration of new information, facilitating monitoring, intervention, and the application of discount factors, which are typical in sequential analyses. The R package `kDGLM` is available for direct use by applied researchers, facilitating the implementation of the method for specific k -parametric dynamic generalised models.

Keywords: Bayesian analysis, Dynamic models, Information geometry, Monitoring and intervention, Sequential analysis.

S.1 Results for the simulated example of the dynamic multinomial model

In this section, we evaluate the effect of varying sample sizes T ($T = 2, 5, 20, 50$), as well as different specifications of the number of allocation categories, N , on the approximated inference produced by the sequential kDGLM proposal. We consider synthetic data simulated as described in Section ?? and compare the results of our proposed method to those obtained via non-sequential NUTS in Stan.

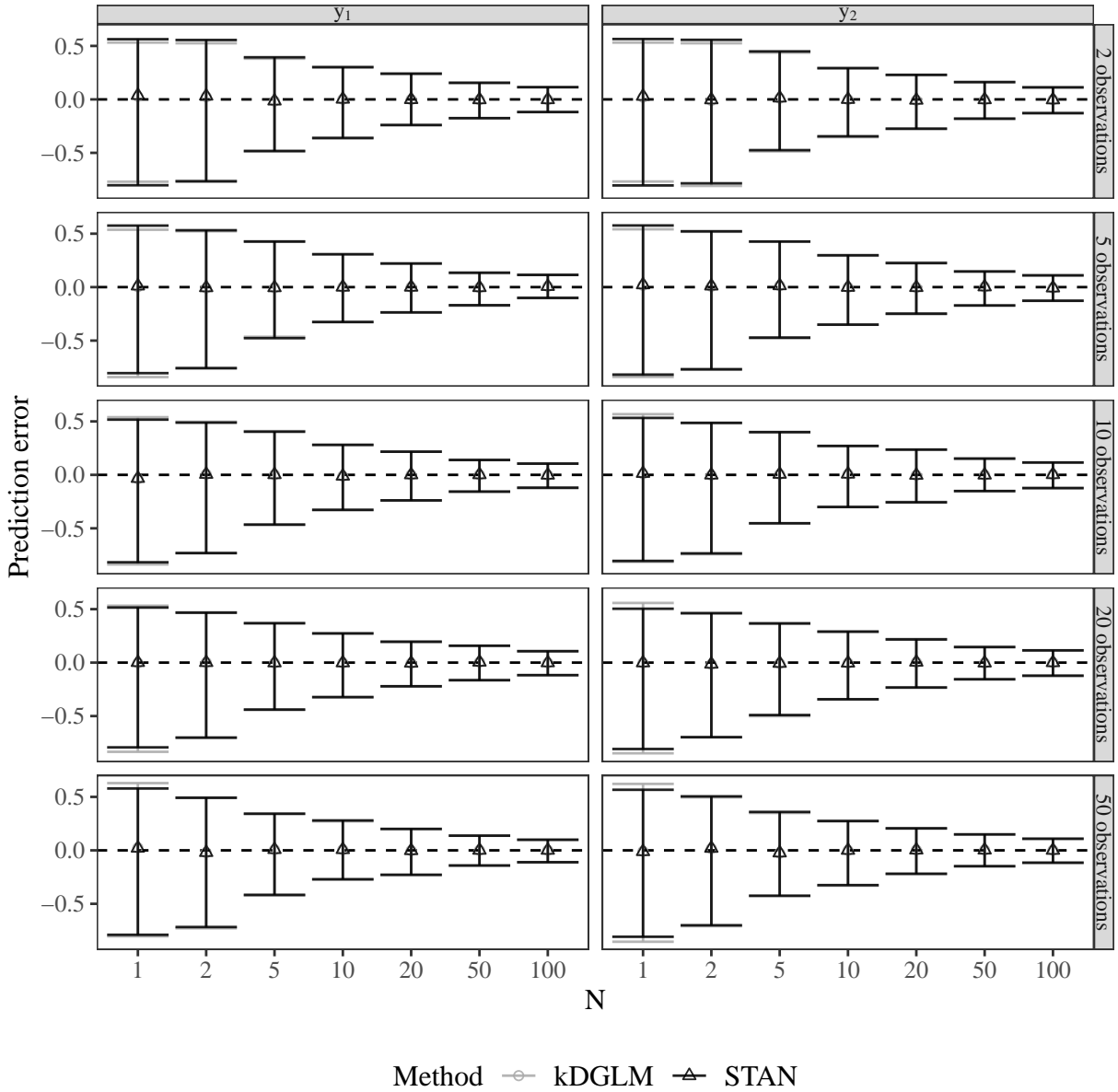


Figure S.1: The bias for the one-step-ahead prediction for $Y_{1,T+1}$ and $Y_{2,T+1}$. Gray circles and black triangles represent the average bias among all samples, while the error bars represent the 0.975 and 0.025 quantiles. To facilitate visualization, the bias is divided by N . Gray: Sequential kdGLM. Black: Stan.

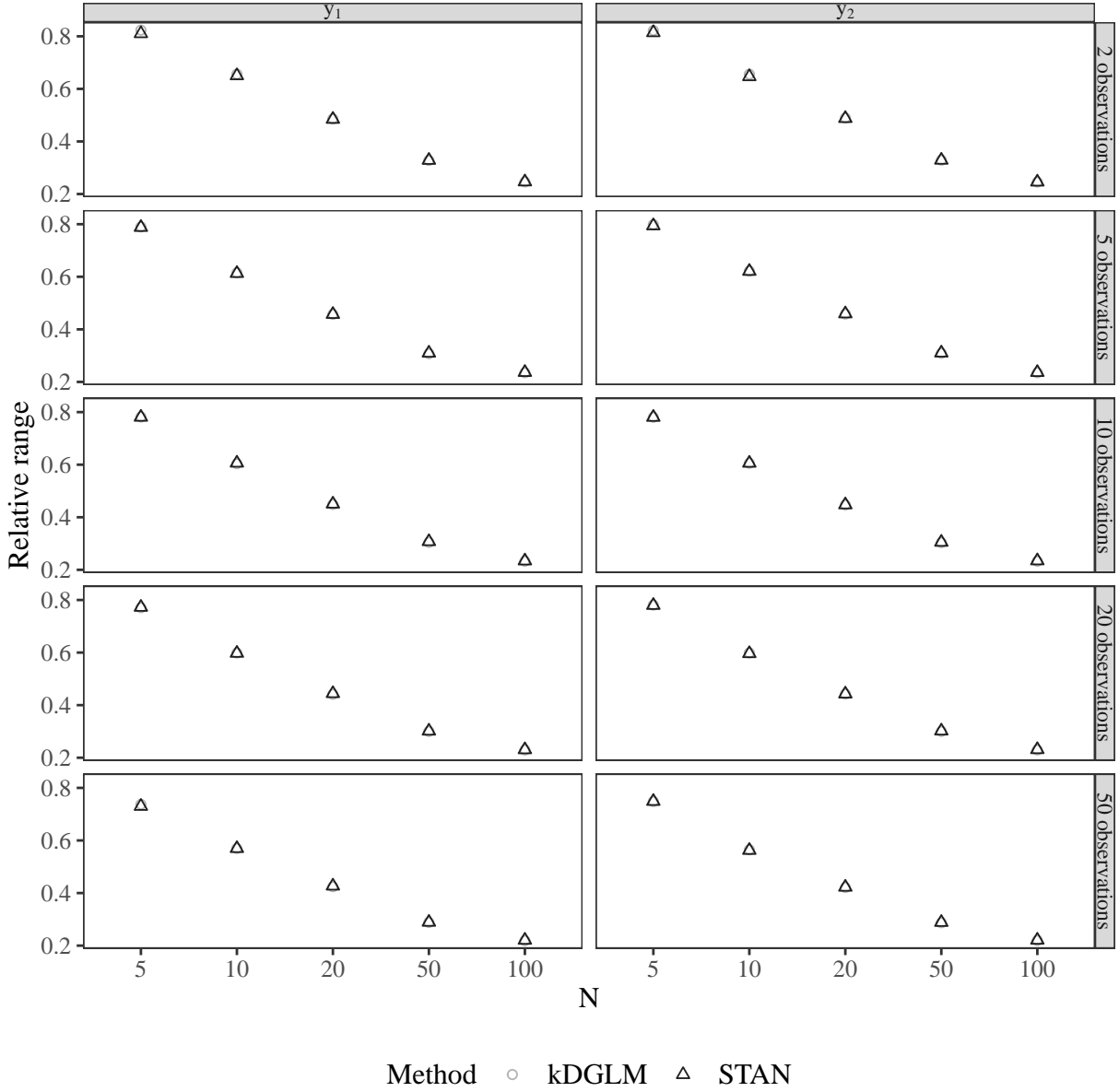


Figure S.2: The range of the 95% credibility interval for one-step-ahead prediction for $Y_{1,T+1}$ and $Y_{2,T+1}$. Gray circles: Sequential kDGLM. Black triangles: Stan.

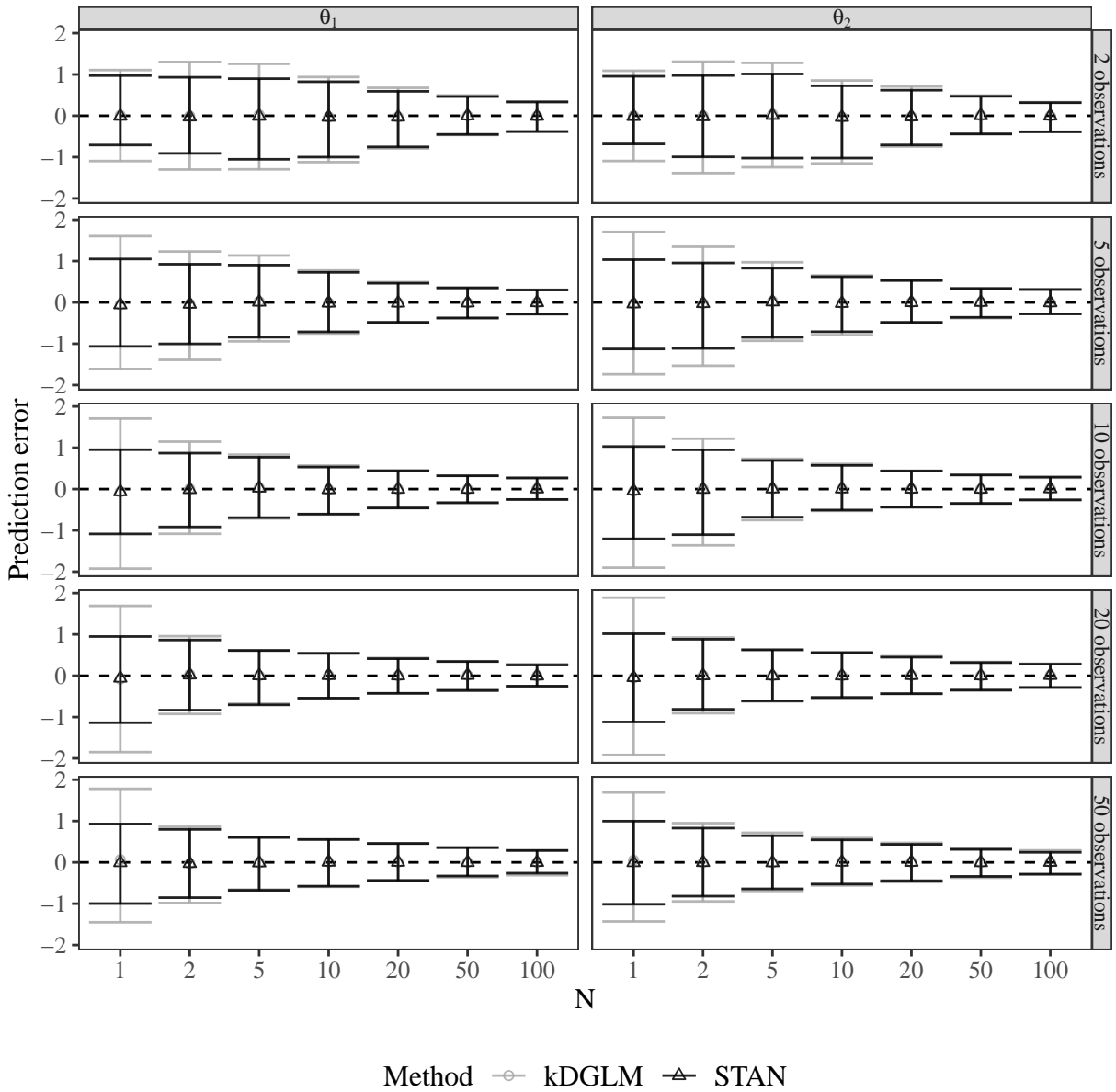


Figure S.3: The bias for the latent states at time T . Gray circles and black triangles represent the average bias among all samples, while the error bars represent the 0.975 and 0.025 quantiles. Gray: Sequential kdGLM. Black: Stan.

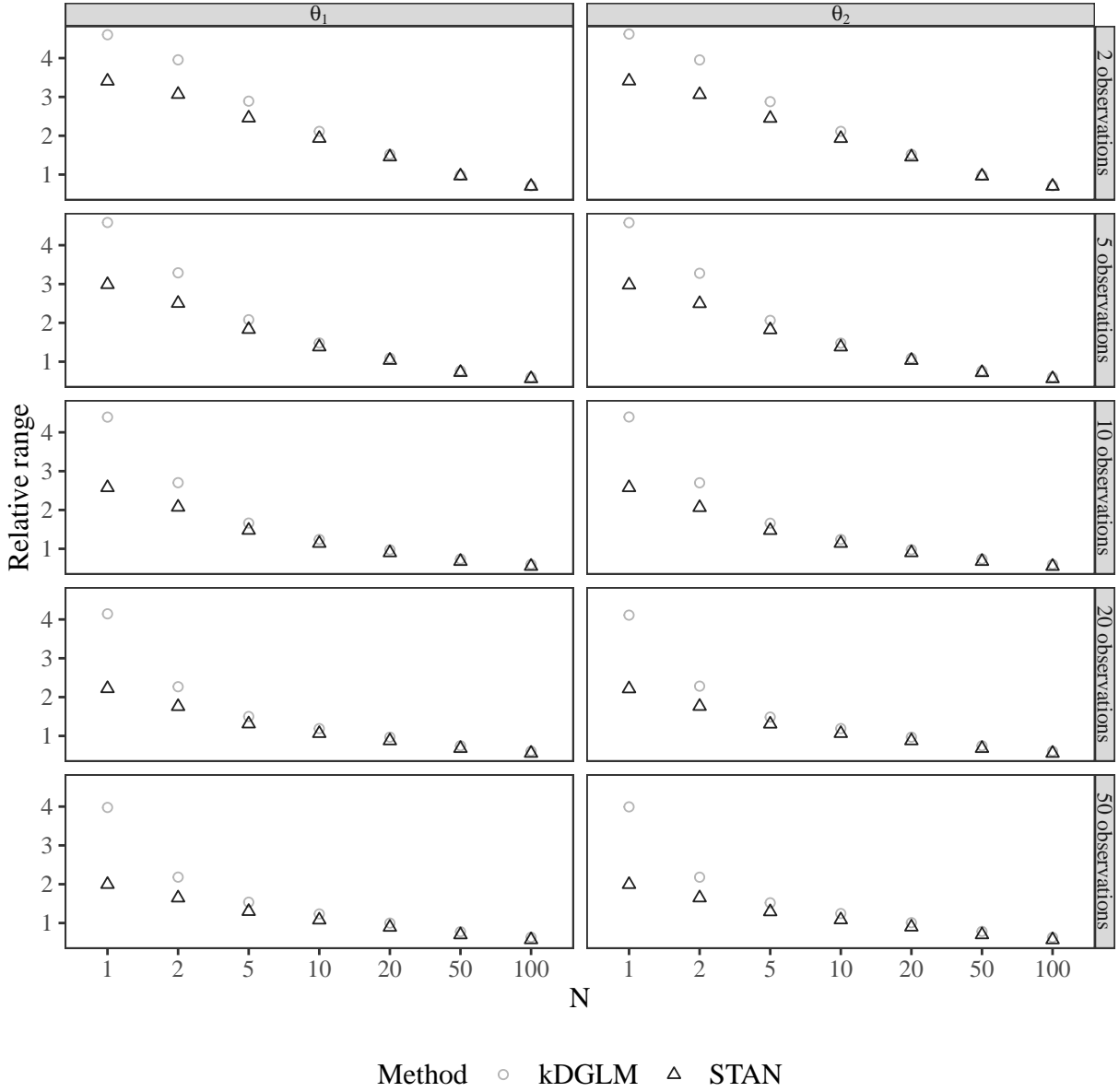


Figure S.4: The range of the 95% credibility interval for the latent states at at time T . Gray: Sequential kDGLM. Black: Stan.

S.2 Analytical development of the proposed method for normal and gamma members of the exponential family

This section provides a detailed description of the analytical developments involved in updating information for the normal and gamma distributions within the kDGLM sequential method. These are the sole instances presented in this work in which the application of the suggested methodology is not straightforward. The outlined procedures are executed at each time point t during the information updating process.

Normal distribution with unknown mean and precision: Consider the general formulation and parametrization defined in Section ?? for the normal model with dynamic predictive structure for the mean and precision. Since $\boldsymbol{\lambda} \sim N_2(\mathbf{f}, \mathbf{Q})$, a system of equations in τ remains to be solved, that is, $E_q[\mathbf{H}_q(\mu, \phi)] = E_p[\mathbf{H}_q(\mu, \phi)]$, with q denoting a normal-gamma prior distribution and p , the density implied by the joint normality of the linear predictors for the mean and log-precision. Using the facts that: i) $E_q[\mathbf{H}_q(\mu, \phi)] = \nabla b(\tau_1, \tau_2, \tau_3, \tau_0)$; ii) $E_p[\mathbf{H}_q(\mu, \phi)] = E_{p(\phi)}[E_{p(\mu|\phi)}\mathbf{H}_q(\mu, \phi)]$ which can be obtained by normal conditioning properties; iii) under p , $\phi \sim LN(f_2, q_2)$ and $\ln \phi \sim N(f_2, q_2)$, results in the system:

$$\begin{cases} \frac{(2\tau_0+1)\tau_2^2}{2\tau_1\tau_2^2-8\tau_1^2\tau_3} - \frac{1}{2\tau_1} & = \exp(f_2 + q_2/2)[(f_1 + q_{12})^2 + q_1] \\ \frac{-(2\tau_0+1)\tau_2}{\tau_2^2-4\tau_1\tau_3} & = \exp(f_2 + q_2/2)(f_1 + q_{12}) \\ \frac{4\tau_1(\tau_0+1/2)}{\tau_2^2-4\tau_1\tau_3} & = \exp(f_2 + q_2/2) \\ \gamma(\tau_0 + 1/2) - \ln\left(\frac{\tau_2^2}{4\tau_1} - \tau_3\right) & = f_2 \end{cases}, \quad (\text{S.1})$$

with $\gamma(\cdot)$ denoting the digamma function. This system can be analytically solved, as follows: applying the parametrization:

$$c_0 = -2\tau_1, \quad \mu_0 = -\frac{\tau_2}{2\tau_1}, \quad \frac{d_0}{2} = \frac{\tau_2^2}{4\tau_1} - \tau_3, \quad \frac{n_0}{2} = \tau_0 + 1/2, \quad (\text{S.2})$$

to the third equation in (S.1), it follows that $n_0/d_0 = \exp(f_2 + q_2/2)$. Multiplying the third equation by $-\frac{2\tau_2}{4\tau_1} = \mu_0$ we obtain the second equation in (S.1) resulting in $\mu_0 = f_1 + q_{12}$. Doing some algebra in the first equation of (S.1), it follows that $c_0 = [q_1 \exp(f_2 + q_2/2)]^{-1}$. Finally, applying the approximation $\gamma(u) \approx \ln(u) - 1/(2u)$ to the fourth equation of the

system, results in $n_0 = 2/q_2$. Applying the reparametrization in (S.2) we obtain the following closed analytical expressions:

$$\begin{cases} \tau_0 &= 1/q_2 - 1/2 \\ \tau_1 &= -[2q_1 \exp(f_2 + q_2/2)]^{-1} \\ \tau_2 &= (f_1 + q_{12})[q_1 \exp(f_2 + q_2/2)]^{-1} \\ \tau_3 &= -(f_1 + q_{12})^2[2q_1 \exp(f_2 + q_2/2)]^{-1} - [q_2 \exp(f_2 + q_2/2)]^{-1}. \end{cases}$$

After observing \mathbf{y} , we obtain $\boldsymbol{\tau}^* = (\tau_1^*, \tau_2^*, \tau_3^*, \tau_0^*) = (\tau_1 - 1/2, \tau_2 + y, \tau_3 - y^2/2, \tau_0 + 1/2)$, the updated canonical parameters of a normal-gamma posterior density for (μ, ϕ) , and need to evaluate the parameters $(\mathbf{f}^*, \mathbf{Q}^*)$ of the posterior distribution of the linear predictors that are compatible with them, solving: $E_q[\mathbf{H}_q] = E_p[\mathbf{H}_q]$, now considering that p is a normal-gamma density for (μ, ϕ) and q is a bivariate normal for $(\mu, \ln \phi)$. $\mathbf{H}'_q = (\boldsymbol{\lambda}, \boldsymbol{\lambda}\boldsymbol{\lambda}')$, so the following system is trivially solved:

$$\begin{cases} f_1^* &= -\frac{\tau_2^*}{2\tau_1^*} \\ f_2^* &= \gamma(\tau_0^* + 1/2) - \ln\left(\frac{(\tau_2^*)^2}{4\tau_1^*} - \tau_3^*\right) \\ Q_{11}^* &= \frac{\tau_2^{*2} - 4\tau_1\tau_3}{4\tau_0\tau_1 - 2\tau_1} \\ Q_{12}^* &= 0 \\ Q_{22}^* &= \gamma'(\tau_0^* + 1/2). \end{cases}$$

Notice that, no matter the values of $\tau_0^*, \tau_1^*, \tau_2^*$ and τ_3^* , $Q_{12}^* = 0$, since the parameters that minimize the KL divergence from p to q must satisfy $Cov_p[\mu, \ln(\phi)] = Cov_q[\mu, \ln(\phi)]$ and, as a property of the normal-gamma distribution, we have that (μ, ϕ) are uncorrelated (although not independent), consequently, it can be shown that $(\mu, \ln \phi)$ are also uncorrelated.

Using the reparametrization $c_0^* = -2\tau_1^*$, $\mu_0^* = -\frac{\tau_2^*}{2\tau_1^*}$, $\frac{d_0^*}{2} = \frac{\tau_2^{*2}}{4\tau_1^*} - \tau_3^*$ and $\frac{n_0^*}{2} = \tau_0^* + 1/2$, we obtain:

$$\begin{cases} f_1^* &= \mu_0^* \\ f_2^* &= \gamma(n_0^*/2) - \ln(d_0^*/2) \\ Q_{11}^* &= \frac{d_0^*/2}{c_0^*(n_0^*/2 - 1)} \\ Q_{12}^* &= 0 \\ Q_{22}^* &= \gamma'(n_0^*/2). \end{cases}$$

An important point to discuss is the equation that defines Q_{11}^* . Specifically, notice that Q_{11}^* is not defined for $n_0^* \leq 2$. Indeed, by the Projection Theorem, the parameters

that minimize the KL divergence from p to q must satisfy $Var_p[\mu] = Var_q[\mu]$, but in the conjugated posterior distribution $\mu|\phi \sim N(\mu_0^*, (c_0^*\phi)^{-1})$ and $\phi \sim \mathcal{G}(n_0^*/2, d_0^*/2)$, which implies that $\mu \sim t\left(n_0^*, \mu_0^*, \frac{d_0^*/2}{c_0^*n_0^*/2}\right)$, so that when $n_0^* \leq 2$, $Var_p[\mu] = +\infty$, and the system $E_q[\mathbf{H}_q] = E_p[\mathbf{H}_q]$ has no valid solutions. Indeed, one can always reduce the KL divergence from p to q by increasing Q_{11}^* . This situation is quite undesirable since it compromises the use of our proposed methodology. Yet, we can restrict the parameter space for the normal posterior distribution to guarantee that, inside that restricted space, we always have a minimum for the divergence from p to q . A natural restriction for the parameter space is to set $Q_{11}^* = \frac{d_0^*/2}{c_0^*n_0^*/2}$, since:

- This restriction guarantees that the scale parameter for the marginal distribution of μ is identical in both the normal and the conjugated distribution.
- for a large value of n_0^* (which we expect to have for a reasonable sample size), $\frac{d_0^*/2}{c_0^*n_0^*/2} \approx \frac{d_0^*/2}{c_0^*(n_0^*/2-1)}$, i.e., for large values of n_0^* this restriction has no significant effect, in the sense that the optimum in the restricted space will be very close to the global optimum.
- $Q_{11}^* = \frac{d_0^*/2}{c_0^*n_0^*/2}$ becomes numerically well behaved for any possible value of n_0^* , since, after updating our knowledge of μ , it is guaranteed that $n_0^* \geq 1$, avoiding a division by values close to zero.

Gamma distribution with unknown shape α : Let $\boldsymbol{\eta} = (\alpha, \mu)$ and $(y|\boldsymbol{\eta}) \sim \mathcal{G}(\alpha, \alpha/\mu)$, $\alpha, \mu > 0$. Unlike other particular cases discussed in this work, the normalising constant of the joint prior for the pair (α, μ) is unknown and the conjugate prior is $\pi(\alpha, \mu) \propto \exp\left\{\tau_0\left(\alpha \ln\left(\frac{\alpha}{\mu}\right) - \ln(\Gamma(\alpha))\right) + \tau_1\alpha - \tau_2\frac{\alpha}{\mu}\right\}$. Consider a vector of linear predictors $\boldsymbol{\lambda}' = (\lambda_1, \lambda_2) = (\ln(\mu), \ln(\phi)) = (F_1'\theta_1, F_2'\theta_2)$. Following Algorithm ??:

- Step 1: Given posterior moments for the states, obtain the prior moments of $\boldsymbol{\lambda} \sim N(\mathbf{f}, \mathbf{Q})$.
- Step 2.1: Obtain the conjugate prior sufficient statistics vector:

$$\mathbf{H}_q = \left(\alpha \ln(\mu) - \alpha \ln(\alpha) + \ln(\Gamma(\alpha)), \alpha, \frac{\alpha}{\mu}\right)'$$
- Step 2.2: Solve the system $E_q[\mathbf{H}_q(\boldsymbol{\eta})] = E_p[\mathbf{H}_q(\boldsymbol{\eta})]$, where p is the prior density induced by the normal specification for the linear predictors. It is easily seen that $\mu|\alpha \sim \mathcal{IG}(\tau_0\alpha - 1, \alpha\tau_2)$

where \mathcal{IG} denotes the inverse gamma density, if $\alpha > 1/\tau_0$. Using the fact that $E_q[\mathbf{H}_q] = E_q[E_q[\mathbf{H}_q|\alpha]]$ and that $E_q[\ln(\mu)|\alpha] = -\gamma(\tau_0\alpha - 1) + \ln(\alpha\tau_2)$, it follows that:

$$\begin{aligned} E_q\left[\frac{\alpha}{\mu}\right] &= E_q\left[\alpha E_q\left[\frac{1}{\mu}|\alpha\right]\right] = E_q\left[\alpha \frac{\tau_0\alpha + 1}{\alpha\tau_2}\right] = \frac{\tau_0 E_q[\alpha] - 1}{\tau_2}; \\ E_q[\alpha \ln(\mu)] &= E_q[\alpha E_q[\ln(\mu)|\alpha]] = E_q[\alpha(-\gamma(\tau_0\alpha + 1) + \ln(\alpha\tau_2))]. \end{aligned}$$

Assuming $E_p[H_q]$ known, and using the fact that $E_q[\alpha] = E_p[\alpha]$ (from the system to be solved), it follows that $\tau_2 = \frac{\tau_0 E_q[\alpha] - 1}{E_q[\frac{\alpha}{\mu}]}$. One can trivially find that $E_q[\alpha \ln(\mu) - \alpha \ln(\alpha) + \ln(\Gamma(\alpha))] = E_q[\ln(\Gamma(\alpha) - \alpha\gamma(\tau_0\alpha + 1))] + E_q[\alpha] \ln(\tau_2)$. Thus, $E_q[\mathbf{H}_q]$ can be expressed in terms of expected values which solely depend on the marginal prior for α : $\pi(\alpha) = \int_0^{+\infty} \pi(\alpha, \mu) d\mu \propto \frac{\alpha^{\tau_0\alpha}}{\alpha^{-\tau_0} \Gamma(\alpha+1)^{\tau_0}} \frac{\Gamma(\tau_0\alpha+1)}{\alpha^{\tau_0\alpha+1} \tau_2^{\tau_0\alpha+1}} \exp\{\tau_1\alpha\}$. Applying Stirling's formula $\Gamma(x+1) \approx \sqrt{2\pi x} \left(\frac{x}{e}\right)^x$ to this last expression results in: $\pi(\alpha) \propto \alpha^{\frac{\tau_0-1}{2}-1} \exp\{-[\tau_0 \ln(\frac{\tau_2}{\tau_0}) - \tau_1]\alpha\}$, that is, α approximately follows a $\mathcal{G}\left(\frac{\tau_0+1}{2}, \tau_0 \ln\left(\frac{\tau_2}{\tau_0}\right) - \tau_1\right)$ marginal conjugate prior, so that:

$$E_q[\alpha] = \frac{\tau_0 + 1}{2\left(\tau_0 \ln\left(\frac{\tau_2}{\tau_0}\right) - \tau_1\right)}.$$

Using a second order approximation for the digamma function, $\gamma(x) \approx \ln(x) - \frac{1}{2x} - \frac{1}{12x^2}$, and the fact that $\gamma(x+1) = \gamma(x) + \frac{1}{x}$ results in:

$$\begin{aligned} -\alpha\gamma(\tau_0\alpha + 1) &= -\alpha\left(\gamma(\tau_0\alpha) + \frac{1}{\tau_0\alpha}\right) \\ &\approx -\alpha\left(\ln(\tau_0\alpha) - \frac{1}{2\tau_0\alpha} - \frac{1}{12\tau_0^2\alpha^2} + \frac{1}{\tau_0\alpha}\right) \\ &\approx -\alpha \ln(\alpha) - \alpha \ln(\tau_0) + \frac{1}{12\tau_0^2\alpha} - \frac{1}{2\tau_0}. \end{aligned}$$

Once again using a second order approximation for the digamma function and the fundamental theorem of Calculus:

$$\ln(\Gamma(x)) = \int_1^x \gamma(t) dt \approx \int_1^x \ln(t) - \frac{1}{2t} - \frac{1}{12t^2} dt = x \ln(x) - x - \frac{1}{2} \ln(x) + \frac{1}{12x} + \frac{11}{12}.$$

The stated facts allow us to calculate the expected value of the remaining sufficient statistic, resulting in the following system to be solved:

$$\left\{ \begin{array}{l} \mathbb{E}_p [(\alpha \ln(\mu) - \alpha \ln(\alpha) + \ln(\Gamma(\alpha)))] \\ \exp\{f_1 + Q_{11}/2\} \\ \exp\{f_1 - f_2 + Q_{11}/2 + Q_{12} + Q_{22}/2\} \end{array} \right. = \begin{array}{l} \frac{\tau_0+1}{2(\tau_0 \ln(\frac{\tau_2}{\tau_0}) - \tau_1)} (\ln(\tau_2/\tau_0) - 1) - \frac{1}{2} \psi\left(\frac{\tau_0+1}{2}\right) \\ + \frac{1}{2} \ln\left(\tau_0 \ln\left(\frac{\tau_2}{\tau_0}\right) - \tau_1\right) + \frac{\tau_0+1}{\tau_0-1} \frac{\ln\left(\frac{\tau_2}{\tau_0}\right) - \tau_1}{6} \\ + \frac{11}{12} - \frac{1}{2\tau_0} \\ \frac{\tau_0+1}{2(\tau_0 \ln(\frac{\tau_2}{\tau_0}) - \tau_1)} \\ \frac{\tau_0(\tau_0+1)-1}{\tau_2 2(\tau_0 \ln(\frac{\tau_2}{\tau_0}) - \tau_1)} \end{array}$$

with $\mathbb{E}_p [(\alpha \ln(\mu) - \alpha \ln(\alpha) + \ln(\Gamma(\alpha)))]$ evaluated by numerical integration, with negligible cost.

- Step 3: Update the hyperparameters of the conjugate specification: $\boldsymbol{\tau}^* = (\tau_0^*, \tau_1^*, \tau_2^*) = (\tau_0 + 1, \tau_1 + \ln(y), \tau_2 + y)$.
- Step 4.1: Let q denote a multivariate normal density for the vector of linear predictors, with sufficient statistics vector: $\mathbf{H}'_q = (\boldsymbol{\lambda}, \boldsymbol{\lambda}\boldsymbol{\lambda}')$.
- Step 4.2: Solve the system $E_q[\mathbf{H}_q(\boldsymbol{\lambda})] = E_p[\mathbf{H}_q(\boldsymbol{\lambda})]$, where p is the updated distribution, obtaining: $f_1^* = E_p[\ln(\mu)]$, $f_2^* = E_p[\ln(\alpha)]$; $Q_{11}^* = V_p[\ln(\mu)]$, $Q_{12}^* = Cov_p[\ln(\mu), \ln(\alpha)]$, $Q_{22}^* = E_p[\ln(\alpha)]$. Using the fact that α approximately follows a $\mathcal{G}\left(\frac{\tau_0^*+1}{2}, \tau_0^* \ln\left(\frac{\tau_2^*}{\tau_0^*}\right) - \tau_1^*\right)$ conjugate marginal posterior, it follows that:

$$\begin{aligned} E_p[\ln(\alpha)] &\approx \gamma\left(\frac{\tau_0^*+1}{2}\right) - \ln\left(\tau_0^* \ln\left(\frac{\tau_2^*}{\tau_0^*}\right) - \tau_1^*\right) \\ V_p[\ln(\alpha)] &\approx \gamma'\left(\frac{\tau_0^*+1}{2}\right). \end{aligned}$$

Since, *a posteriori*, $\mu|\alpha \sim \mathcal{IG}(\tau_0^*\alpha + 1, \alpha\tau_2^*)$, it follows that:

$$\begin{aligned} E_p[\ln(\mu)] &= E_p[E_p[\ln(\mu)|\alpha]] = -E_p[\gamma(\tau_0^*\alpha + 1) - \ln(\alpha\tau_2^*)]; \\ V_p[\ln(\mu)] &= V_p[\ln(1/\mu)] = E_p[V_p[\ln(1/\mu)|\alpha]] + V_p[E_p[\ln(1/\mu)|\alpha]] \\ &= E_p[\gamma(\tau_0^*\alpha + 1)] + V_p[\gamma(\tau_0^*\alpha + 1) - \ln(\alpha\tau_2^*)]; \\ E_p[\ln(\alpha) \ln(\mu)] &= -E_p[\ln(\alpha) \ln(1/\mu)] = -E_p[\ln(\alpha) E_p[\ln(1/\mu)|\alpha]] \\ &= -E_p[\ln(\alpha)(\gamma(\tau_0^*\alpha + 1) - \ln(\alpha\tau_2^*))]. \end{aligned}$$

All the integrals involved in the expected values above are evaluated by numerical integration, with negligible cost.

- Step 5: The updated moments of the states $\boldsymbol{\theta}$ are trivially obtained, applying normal distribution properties.

Since the normalizing constant of the conjugate prior is unknown, we trivially obtain a sample from the predictive distribution, first sampling from the posterior $\boldsymbol{\lambda}$ and then sampling from the observational distribution of $y^*|\boldsymbol{\lambda}$. Since we assume that $\boldsymbol{\lambda}$ follows a multivariate normal distribution, the computational cost of this process is negligible.

S.3 Comparison between kDGLM and NUTS via Stan for the stochastic volatility example

Section ?? presents a comparison between the results obtained using the sequential kDGLM method proposed in this work and those from a NUTS scheme implemented via Stan. The comparison relies on synthetic, artificially generated data. As discussed, the differences observed in the inference produced by the two methods are largely attributable to the linearization employed for sequential inference for the autoregressive parameter γ in the kDGLM method.

In Figure S.5, we display the inference results under both methods, kDGLM and NUTS, with the parameter γ fixed at its true value. As shown, the two methods yield nearly identical results. Therefore, for models where the evolution matrix \mathbf{G} is known, the kDGLM method is expected to produce inferences closely aligned with those generated by Markov Chain Monte Carlo schemes.

S.4 A Poisson model for quarterly sales

This section presents a model for univariate, uniparametric responses. Unlike methods based on local levels, where only the level evolves dynamically, our goal is to emphasise the versatility of the proposed method, which allows the assignment of temporal dynamics for all latent components of the predictor. We highlight the lower computational cost involved in our proposal, in comparison with a local level method (Gamerman et al., 2013). Finally, we show that, in the single parameter case, our method is equivalent to the one suggested by West et al. (1985), in terms of model flexibility, computational cost and resulting inference.

For the analytical development of our proposed approach for Poisson responses, we follow the steps described in Section ?. Let $y|\eta \sim Po(\eta)$, $\eta > 0$. The conjugate prior is a gamma

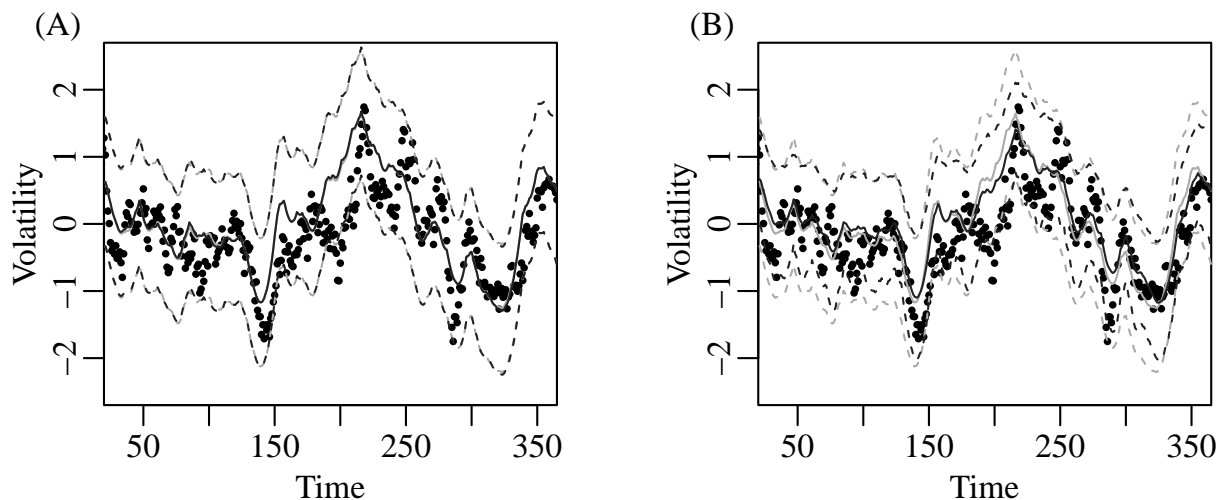


Figure S.5: Comparison of smoothed means (solid lines) and credible intervals (dashed lines) for volatility estimation from synthetic data, with fixed autoregressive parameter γ . The solid circles indicate theoretical volatilities. (A): results of the proposed sequential approach for normal (grey) and gamma (black) formulations. (B): comparison of normal formulation using the sequential approach (grey) and NUTS via Stan (black).

density $q(\eta|\boldsymbol{\tau}) = \frac{1}{\eta} \exp[\tau_1 \log(\eta) - \tau_0 \eta - b(\tau_0, \tau_1)]$, where $b(\tau_0, \tau_1) = \log(\Gamma(\tau_1)) - \tau_1 \log(\tau_0)$. Consider the linear predictor $\lambda = \log(\eta) = \mathbf{F}'\boldsymbol{\theta}$ and the conjugate prior sufficient statistics vector: $\mathbf{H}_q(\eta) = (\log(\eta), \eta)'$. Following Algorithm ?? and using the fact that $E_q[\mathbf{H}_q(\eta)] = \nabla b(\tau_0, \tau_1)$ as well as approximation (??) for the digamma function, the solution of the system $E_q[\mathbf{H}_q(\eta)] = E_p[\mathbf{H}_q(\eta)]$ in Step 2.2 results in $\tau_0 = \tau_1 \exp[-(f + Q/2)]$ and $\tau_1 = (1 + \sqrt{1 + 2Q/3})/(2Q)$. The conjugate prior hyperparameters are updated to $\tau_1^* = \tau_1 + y$ and $\tau_0^* = \tau_0 + 1$. Step 4.2 is completed by solving the system $E_q[\mathbf{H}_q(\boldsymbol{\lambda})] = E_p[\mathbf{H}_q(\boldsymbol{\lambda})]$, where p is the updated distribution, obtaining: $f^* = \gamma(\tau_1^*) - \log(\tau_0^*)$ and $Q^* = \gamma'(\tau_1^*)$.

The updated moments of the states $\boldsymbol{\theta}$ are trivially obtained by applying normal distribution properties and the predictive distribution for y_t is a Poisson-Gamma($\tau_0, \tau_1, 1$), which can be evaluated once step 2.2 is completed.

We apply a Poisson dynamic model to predict a time series of quarterly sales with a growth trend and stochastic seasonal pattern, as detailed in West and Harrison (1997, Chap. 8, p. 268). True data are shown as solid circles in Figure S.6. We compare this with West et al. (1985), using a Poisson log-linear model with linear growth and two pairs of harmonics

for a Fourier description of the seasonal pattern.

Let $y_t|\eta_t \sim \text{Poisson}(\eta_t)$; $\log(\eta_t) = \mathbf{F}'_t\boldsymbol{\theta}_t$; $\boldsymbol{\theta}_t = \mathbf{G}_t\boldsymbol{\theta}_{t-1} + \boldsymbol{\omega}_t$, $\boldsymbol{\omega}_t \sim N(\mathbf{0}, \mathbf{W}_t)$, with $\mathbf{F}'_t = [1, 0, 1, 0, 1, 0]$; $\mathbf{G}_t = \text{diag}[\mathbf{G}_0, \mathbf{G}_1, \mathbf{G}_2]$ and

$$\mathbf{G}_0 = \begin{bmatrix} 1 & 1 \\ 0 & 1 \end{bmatrix}, \mathbf{G}_k = \begin{bmatrix} \cos(kw) & \sin(kw) \\ -\sin(kw) & \cos(kw) \end{bmatrix}, w = 2\pi/4 \text{ and } k = 1, 2.$$

The prior specification is as follows: $\boldsymbol{\theta}_0|D_0 \sim N(m_0 = 0, C_0 = 1)$, and we employ a diagonal block discount factor matrix for \mathbf{W}_t covariance evolution. For the conjugate updating approach of West et al. (1985) we specify the same first- and second-order prior moments. Both methods begin with $\boldsymbol{\theta}_0|D_0$, updated to the prior $\boldsymbol{\theta}_1|D_0$, inducing a predictor's prior structure.

Figure S.6 exhibits smoothed mean responses, illustrating the proposed method's efficiency in managing predictive structures with multiple dynamic components. Our approach accommodates various stochastic patterns typical in real time series while preserving sequential analysis.

We also compare our approach with the local level method proposed by Gamerman et al. (2013), who introduced Gamma Family Dynamic Models (GFDM) integrating Smith and Miller (1986) and Harvey and Fernandes (1989). GFDM combines a local steady structure (a dynamic level) with a fixed-coefficient predictor, applicable to models such as Poisson, gamma, Weibull, and normal, as well as others outside the exponential family. Unlike our model, GFDM does not extend beyond the level dynamics. To align with our model's structure, we define regressors $x_1 = t, x_2 = \cos(wt), x_3 = \sin(wt), x_4 = \cos(2wt), x_5 = \sin(2wt)$, where $t = 1, \dots, 35$ and $w = 2\pi/4$, applying the local level approach of Gamerman et al. (2013) to the following model: $y_t|\eta_t \sim \text{Poisson}(\eta_t)$; $\eta_t = \alpha_t \exp(\beta_1 x_{1t} + \beta_2 x_{2t} + \beta_3 x_{3t} + \beta_4 x_{4t} + \beta_5 x_{5t})$. The model is completed with a $\text{Gamma}(0.34, 0.04)$ prior for η_0 to standardise prior settings across methods and a $\text{Uniform}(0, 1)$ prior to manage the increase in the uncertainty associated with the local level approach's evolution, impacting dynamic level smoothness (Gamerman et al., 2013). Parameters β_k , for $k = 1, \dots, 5$, follow independent $\text{Normal}(0, 1)$ priors. The NGSSEML package (Santos et al., 2021) performed inference with MCMC steps for the static coefficients, and the coda package (Plummer et al., 2006) facilitated convergence diagnosis, burn-in, and thinning. Both our method and that of West et al. (1985) involving conjugate updating provided smoothed estimates and

predictions in under one second. Figure S.6 illustrates the expected value of the smoothed mean response function obtained from our method and Gamerman et al. (2013), excluding West et al. (1985)’s results, which are almost identical to ours. Our method and conjugate updating do not require sampling, resulting in computational efficiency, in contrast to Gamerman et al. (2013)’s local level method, which took 818.803 seconds (effective sample size 1,700), compared to 0.024 second for our approach and West et al. (1985) (Table S.1).

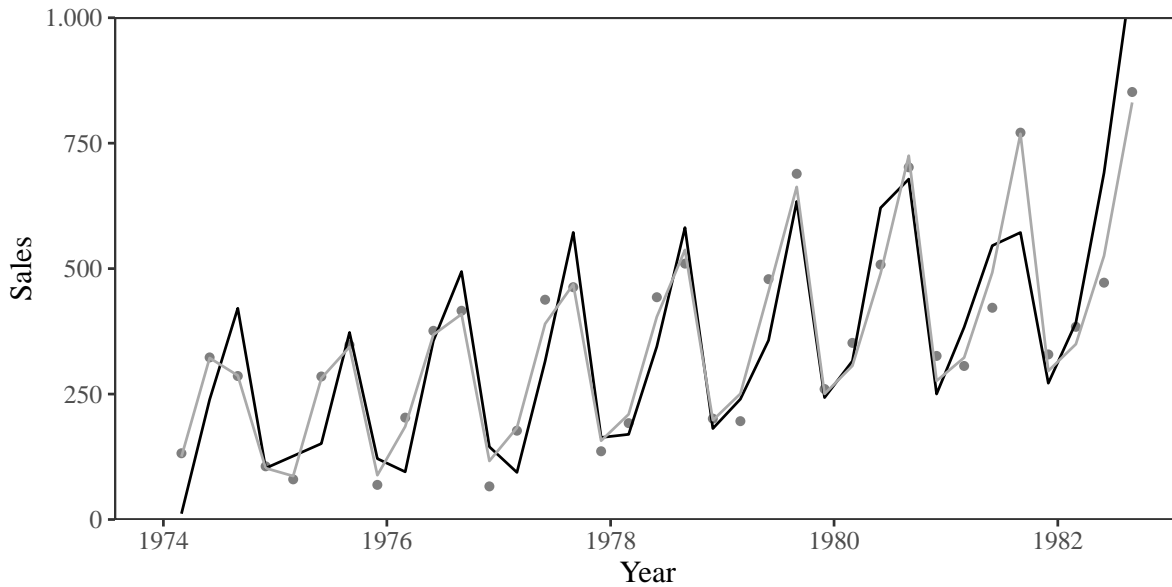


Figure S.6: Quarterly sales: observed time series (solid circles) and the expected value of the smoothed mean response function via sequential kDGLM (solid grey line) and local level method (solid black line).

Metric	Local Level	Conjugate Update	kDGLM
Mean Absolute Error	82.323	27.21166	26.86886
Relative Absolute Error	0.2661	0.1084	0.1077
Log Predictive Likelihood	-214.006	-	-148.8231
Computational time*	818.803s	0.024s	0.024s

Table S.1: Model comparison based on the smoothed mean response function and several metrics. *Time measured using R 4.2.0 running Windows 10 x64 (build 19044) in an Intel(R) Core™ i7-8700K CPU @ 3.70GHz with 16 GB RAM @ 2400 MHz.

According to comparison of the metrics in Table S.1, conjugate updating and our sequen-

tial approach are nearly equivalent. The local level model with deterministic seasonality, which is adjustable by the method proposed by Gamerman et al. (2013), achieved the weakest performance in terms of computational time, as well as regarding fitting and prediction, exhibiting higher uncertainty of smoothed expected values. Unlike West et al. (1985), our information geometry approach enables log predictive likelihood evaluation, which is an inherent advantage. The local level approach lacks seasonal component dynamics, as shown in Figure S.7, where the trend fit by Gamerman et al. (2013)’s method “attempts to compensate” for seasonal inflexibility, showing that our method allows for models that capture structural components with greater precision.

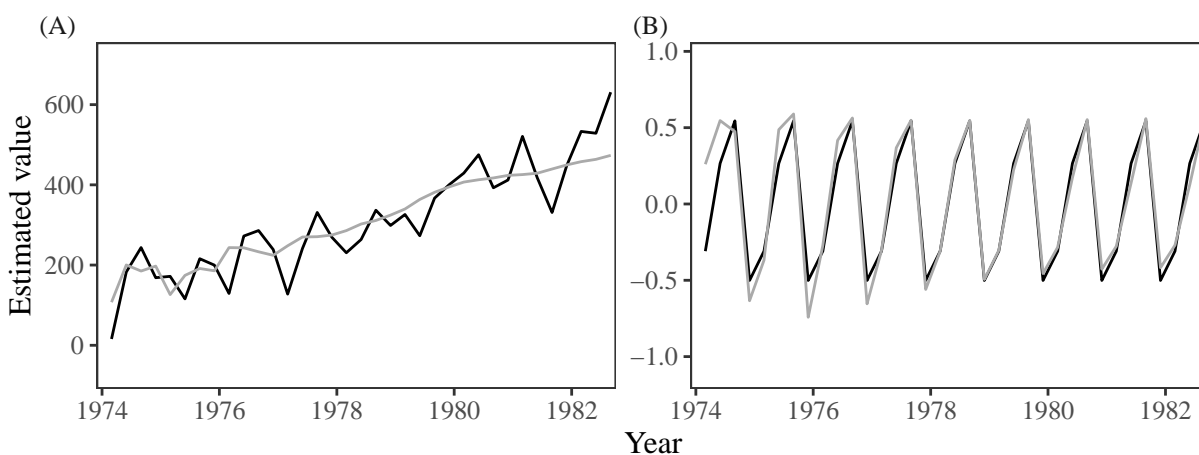


Figure S.7: Structural decomposition - smoothed mean for seasonal and trend components: kDGLM (grey) and local level (black).

References

- Gamerman, D., dos Santos, T. R., and Franco, G. C. (2013). A non-Gaussian family of state-space models with exact marginal likelihood. *Journal of Time Series Analysis*, 34(6):625–645.
- Harvey, A. C. and Fernandes, C. (1989). Time series models for count or qualitative observations. *Journal of Business & Economic Statistics*, 7(4):407–417.

- Plummer, M., Best, N., Cowles, K., and Vines, K. (2006). Coda: Convergence diagnosis and output analysis for mcmc. R News, 6(1):7–11.
- Santos, T. R., Franco, G. C., and Gamerman, D. (2021). NGSSEML: Non-Gaussian state space with exact marginal likelihood. R Journal, 13:111.
- Smith, R. and Miller, J. (1986). A non-Gaussian state space model and application to prediction of records. Journal of the Royal Statistical Society. Series B (Methodological), 48(1):79–88.
- West, M. and Harrison, P. J. (1997). Bayesian Forecasting and Dynamic Models. Springer, New York, NY.
- West, M., Harrison, P. J., and Migon, H. S. (1985). Dynamic generalized linear models and Bayesian forecasting. Journal of the American Statistical Association, 80(389):73–83.